IEEE Access
Multidisciplinary : Rapid Review : Open Access Journal

Received March 13, 2020, accepted March 28, 2020, date of publication April 6, 2020, date of current version April 24, 2020.
Digital Object Identifier 10.1109/ACCESS.2020.2986058

Research on Satisfactory Integrated Design of Event-Triggered Fault Accommodation and Network Communication Saving for NCSs With Actuator Saturation Under Non-Uniform Transmission

YAJIE LI AND WEI LI
College of Electrical and Information Engineering, Lanzhou University of Technology, Lanzhou 730050, China
Key Laboratory of Gansu Advanced Control for Industrial Processes, Lanzhou University of Technology, Lanzhou 730050, China
National Demonstration Center for Experimental Electrical and Control Engineering Education, Lanzhou University of Technology, Lanzhou 730050, China
Corresponding author: Wei Li (liwei@lut.edu.cn)

This work was supported in part by the National Natural Science Foundation of China under ''Research on co-design of discrete event-triggered communication and robust fault-tolerant control for networked control system'' (Grant No. 61364011), ''Research on the triggering strategy and security control of networked multi-rate sampling system under the denial of service attacks'' (Grant No. 61863026).

ABSTRACT Under the non-uniform transmission period, the satisfactory integrated design problem combining active fault-tolerant control and network communication saving was studied for nonlinear network control systems (NCSs) with actuator saturation constraints based on discrete event-triggered communication scheme (DETCS). First, the model of a non-uniform transmission closed-loop fault system was established, which includes the network attribute, actuator saturation constraints, estimation value of fault and state, event-triggered condition, disturbance information and so on. Second, the method of fault estimation with H_∞-performance was proposed by a continuous time state observer. Furthermore, a satisfactory integrated design method integrating event-triggered fault accommodation and network communication saving was given for non-uniform transmission nonlinear NCSs with α-stability and H_∞/H_2 performance. Finally, a MATLAB simulation was conducted to verify the effectiveness and feasibility of the proposed method based on a nonlinear NCS example. In order to reflect the real network transmission circumstances fully, a semi entity experimental platform was also built to verify the effectiveness and feasibility of the proposed method.

INDEX TERMS Active fault-tolerant control, actuator saturation, integrated design, event-triggered fault accommodation, non-uniform transmission.

I. INTRODUCTION

With the increasing scale and complexity of networked control systems (NCSs), the fault-tolerance ability is no longer the luxury property of NCSs, and it will become an essential feature to ensure that the system performance is maintained under all eventualities [1]. Therefore, as an important technology for improving system safety and reliability [2], the fault-tolerant control of NCSs is attracting increasing attention and some outstanding research results [3]–[5] have been achieved in recent years. In actual industry processes, the controlled plant is often more or less subject to nonlinear properties, which leads to a substantial amount of nonlinear controlled plant. As nonlinear NCSs have some complex properties and some unique attributes derived from network transmission media, the fault-tolerant design of nonlinear NCSs is becoming more and more difficult and challenging. Thus such issues have become the focus of research [6], [7] in academia. Moreover, under the premise of ensuring fault-tolerant performance and stability for nonlinear NCSs, some scholars have studied the fault-tolerant control with other performance index constraints [8], [9], such as pole assignment, α-stability, H_∞-disturbance rejection, general H_2-performance, and so on.

In the research on fault-tolerant control, most of the literature is based on the periodic time-triggered communication scheme (PTTCS) for system analysis and synthesis. The PTTCS is easy to design and apply, but has some disadvantages, such as wasting network resources, the separation between control and communication, and so on.

The associate editor coordinating the review of this manuscript and approving it for publication was Lin Wang.

In recent years, some scholars have introduced a new kind of communication scheme, known as the discrete event-triggered communication scheme (DETCS) [10], [11], into the fault-tolerant control of nonlinear NCSs, and they have achieved good application results [12]–[16]. The DETCS only transmits the system data that satisfies the event-triggered condition just at the discrete instant, while the PTTCS transmits system data at every sampling instant. Considering the probability of sensor and actuator faults, [13] studied the problem of reliable control for NCSs. Under the DETCS, the authors of [14] researched the robust fault-tolerant control problem for uncertain nonlinear NCSs with actuator saturation and actuator faults.

Based on the DETCS, the results of fault-tolerant control of nonlinear NCSs are mostly based on the related method of passive fault-tolerant control. However, results related with the active fault-tolerant control method have not been much discussed. In actual application, active fault-tolerant control not only has some advantages, such as the high flexibility of dealing with different kinds of fault, and the optimal performance for fault closed-loop system, but also has a less conservative controller design method compared with passive fault-tolerant control [17]–[19]. Therefore, under the DETCS, the research about the integrated design of active fault-tolerant control and communication resource saving is a problem worth studying. If we can achieve some advances in this subject, then we can attain the goal of improving the fault-tolerant performance of nonlinear NCSs, adjusting the trade-off between active fault-tolerant control and communication for nonlinear NCSs.

Under the fault-tolerant framework of nonlinear NCSs in DETCS, the system data that satisfies the selecting condition of an event-generator is transmitted in a non-uniform period. Because the non-uniform transmission period is an integer multiple of the sampling period, we can consider the sampler and event-generator as a visual non-uniform sampler. Then we can study the problem of the non-uniform transmission of nonlinear NCSs under the DETCS by adopting the related method of a non-uniform sampled-data system. There are three methods [20] for studying a non-uniform sampled-data system. One is to transfer the effect generated by the non-uniform update period on the system performance into the effect of the system time-delay, and we can then adopt the mature method of the time-delay system to study the non-uniform transmission problem [21]. This method does not require the discretisation of continuous system objects, or any special handling of the controller. Therefore it has received increasing recognition and recommendation [22].

Inspired by the above problems, the satisfactory integrated design problem combining active fault-tolerant control and network communication resource saving is studied in this paper based on the non-uniform sampled-data system theory for nonlinear NCSs under DETCS. The active fault-tolerant control section includes the continuous time-varying fault estimation, and the satisfactory integrated design between fault accommodation with multi-objective constraints and communication under DETCS. The estimation of continuous time-varying faults and states is based on a continuous time observer.

The main contributions of this paper are as follows:

1) We propose a distributed implementation architecture to solve the integrated design problem combining active fault tolerant control and network communication. In this architecture, the estimation of faults and states is realised by an intelligent sensor, and the fault accommodation and feedback control are realised by the control unit. Both the intelligent sensor and the control unit have independent processing capabilities, and can carry out local application calculations. Therefore, estimation, regulation and control are implemented in a distributed way.

2) We put forward a closed-loop fault system model for nonlinear T-S fuzzy NCS. This model integrates many factors into one framework, such as network attributes, actuator saturation constraints, fault estimation, disturbance information and event-triggered information. In the course of building the model, the time-triggered observer worked under an equal physical sampling period and the event-triggered controller worked under a virtual non-uniform sampling period.

3) We present the fault/state estimation method and integrated design method for nonlinear NCSs with time-varying faults and actuator saturation. The generalised method of estimating states and failures was presented by adopting a continuous time observer under equal physical sampling period. Furthermore, under the non-uniform transmission period, the satisfactory integrated design method combining active fault-tolerant control and network communication was presented for closed-loop failure NCSs with multi-objective constraints.

4) We not only perform a MATLAB simulation, but also build a semi entity experimental platform and conduct related experiments. In order to fully reflect the real network transmission circumstances, we build this platform based on the campus LAN. This platform is used for verifying the effectiveness and feasibility of the proposed method, and the experiment can improve the engineering practicability of theoretical methods.

Notation: R^n and $R^{m\times n}$ denote the n-dimensional Euclidean space and the set of all $m \times n$ real matrices, respectively. $\boldsymbol{A} > 0$ and $\boldsymbol{A} < 0$ represent positive and negative definiteness, respectively, and $\boldsymbol{A}^T$ denotes the transpose of matrix $\boldsymbol{A}$. The notation $\|\cdot\|$ stands for the 2-norm. In symmetric block matrices, the notation $*$ is used to indicate a term that is induced by symmetry. The $diag\{\cdots\}$ represents the block-diagonal matrix.

II. ESTABLISHMENT OF CLOSED LOOP MODEL

A. SYSTEM DESCRIPTION

With the T-S fuzzy model it is easy to reflect the system dynamic performance, and it has been widely used by many scholars for describing the nonlinear system model [12], [15]. In different areas, the nonlinear system has different dynamic performance. In view of this characteristic, several local linear models are established using the T-S fuzzy model, and then a complete fuzzy nonlinear model is set up by combining several local linear models based on the membership function. In this paper, the model of a nonlinear networked closed-loop fault system is proposed based on the above concept of model establishment, and the system analysis and synthesis are based on the model.

The typical model of nonlinear NCSs is expressed as follows:

$$\begin{cases} \dot{x}(t) = F(x(t), sat(u(t)), f(t), d(t)) \\ \qquad = f(x(t)) + g(x(t))(sat(u(t)), f(t), d(t)) \\ y(i_k) = C(x(i_k), v(i_k)) \end{cases} \tag{1}$$

where $x(t) \in R^n, u(t) \in R^m, f(t) \in R^{n_f}$ indicate the system state variable, control input, and the unknown continuous time-varying fault, respectively. $d(t) \in L_2[0, \infty)$ is the external disturbance with limited energy. The derivative of $f(t)$ is assumed to be norm bounded, namely, there is a constant f_0 and $\|\dot{f}(t)\| \leq f_0$; $sat(\cdot) : R^m \to R^m$ is the standard saturation function, and $sat(u) = [sat(u_1), \cdots sat(u_m)]^T$, $sat(u_i) = sign(u_i) \min\{1, |u_i|\}$; $x(i_k) \in R^n, y(i_k) \in R^m, v(i_k) \in R^{n_v}$ express the system sampling state, system sampling output, and discrete measurement noise, respectively. $f(x(t)), g(x(t)), C(x(i_k), v(i_k))$ are the nonlinear functions which depend on the state.

Based on the following if-then rule, the nonlinear NCSs with actuator saturation constraints can be described as

If $\theta_1(t)$ is M_{i1} and ... and $\theta_n(t)$ is M_{in}, then

$$\begin{cases} \dot{x}(t) = \boldsymbol{A}_i x(t) + \boldsymbol{B}_i sat(u(t)) + \boldsymbol{E}_{di} d(t) + \boldsymbol{E}_{fi} f(t) \\ y(i_k) = \boldsymbol{C}_i x(i_k) + \boldsymbol{D}_{vi} v(i_k) \end{cases} \tag{2}$$

where $i = 1, 2, \cdots, r$, r is the rule number of the if-then; $M_{is}(i = 1, 2, \cdots, r; s = 1, 2, \cdots, n)$ is the fuzzy set, and $\theta(t) = [\theta_1(t), \ldots, \theta_n(t)]^T$ expresses the fuzzy premise variable; $\boldsymbol{A}_i \in R^{n\times n}, \boldsymbol{B}_i \in R^{n\times n_u}, \boldsymbol{E}_{di} \in R^{n\times n_d}, \boldsymbol{E}_{fi} \in R^{n\times n_f}, \boldsymbol{C}_i \in R^{n\times n}, \boldsymbol{D}_{vi} \in R^{n\times n_v}$ indicate the system matrix, input matrix, state disturbance matrix, fault coefficient matrix, system output matrix and output disturbance matrix, respectively.

The state equation of the nonlinear system is the weighted average of every output of the sub-system.

$$\begin{cases} \dot{x}(t) = \sum_{i=1}^{r} \mu_i(\theta(t))[A_i x(t) + B_i sat(u(t)) \\ \qquad + \boldsymbol{E}_{di} d(t) + \boldsymbol{E}_{fi} f(t)] \\ y(i_k) = \sum_{i=1}^{r} \mu_i(\theta(t))[\boldsymbol{C}_i x(i_k) + \boldsymbol{D}_{vi} v(i_k)] \end{cases} \tag{3}$$

where $\mu_i(\theta(t)) = \frac{a_i(\theta(t))}{\sum_{i=1}^{r} a_i(\theta(t))} \geq 0$, $\mu_i(\theta(t)) \geq 0$, $\sum_{i=1}^{r} \mu_i(\theta(t)) = 1$, $a_i(\theta(t)) = \prod_{s=1}^{n} M_{is}(\theta_s(t))$, $i = 1, 2, \cdots, r$, and $a_i(\theta(t)) \geq 0$, $\sum_{i=1}^{r} a_i(\theta(t)) > 0$, $(i = 1, 2\cdots, r)$, $M_{is}(\theta_s(t))$ expresses the membership which indicates premise variable $\theta_s(t)$ for fuzzy value M_{is}.

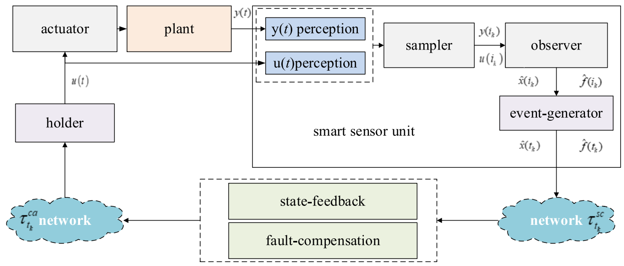

FIGURE 1. The active fault-tolerant control framework of uniform transmission nonlinear NCSs under DETCS.

B. DATA TRANSMISSION MECHANISM OF ACTIVE FAULT-TOLERANT CONTROL

The event-generator is introduced into the active fault-tolerant framework of nonlinear NCSs to solve the network resource wasting problem and integrated design problem, and the structure diagram is shown in Figure 1.

In Figure 1, the sampler is driven by the clock, and the sampling period of the sampler is h. Compared with the sampler of the classical nonlinear NCSs, the estimation information from the observer is required to pass through an event-generator before network transmission, and the function of the event-generator is to select the transmission data that satisfy a certain triggering condition. The event-triggered condition in this paper is expressed as follows:

$$[\hat{x}(i_k) - \hat{x}(t_k)]^T \boldsymbol{\Phi}[\hat{x}(i_k) - \hat{x}(t_k)] \leq \delta \hat{x}^T(t_k)\boldsymbol{\Phi}\hat{x}(t_k) \tag{4}$$

where $\boldsymbol{\Phi}$ is the positive definite symmetric matrix to be designed, and $\delta > 0$ is an event-triggered parameter that is given in advance. $\hat{x}(i_k)$ expresses the estimation value of the state at the latest sampling instant in the backend of the observer. $\hat{x}(t_k)$ indicates the latest estimated value of the state, which is transmitted by computing and comparison in the event-generator at the last instant.

We suppose that $\{i_k\}$ is the sampling instant sequence in the backend of the sampler and $\{t_k\}$ is the data transmission sequence in the backend of the event-generator. In the nonlinear NCSs, the network transmission data can be transmitted to the actuator end after a certain network transmission delay τ_{t_k} at instant t_k. We set $\tau_{t_k} = \tau_{sc}^{t_k} + \tau_c^{t_k} + \tau_{ca}^{t_k}$, where $\tau_{sc}^{t_k}$ is the time-delay between the sensor and controller at instant t_k, $\tau_c^{t_k}$ indicates the computing time-delay in the control unit at instant t_k, and $\tau_{ca}^{t_k}$ expresses the time-delay between the controller and actuator at instant t_k. $\{\bar{t}_k = t_k + \tau_{sc}^{t_k} + \tau_c^{t_k}\}(k = 0, 1, 2, \cdots)$ is the instant sequence of data updating in the backend of the controller. $\{\hat{t}_k = t_k + \tau_{sc}^{t_k} + \tau_c^{t_k} + \tau_{ca}^{t_k}\}(k = 0, 1, 2, \cdots)$ is the instant sequence of data updating in the front end of the actuator.

Furthermore, several assumptions are made as follows: there exist network transmission time-delays $\tau_{sc}^{t_k}$ and $\tau_{ca}^{t_k}$ at the front end and backend of the controller. In the process of calculating the controller, there is computing time-delay $\tau_c^{t_k}$.

Remark 1: This method of analysing the network transmission time-delay can be closer to the actual network transmission, and can make the results of integrated design more practical. However, when we consider the time-delay according to this method, the value of the time-delay will increase, and then the solution space of the gain of the feedback controller in active fault tolerance will be reduced. In order to solve this problem, we adopt some methods to expand the solution space in the subsequent derivation of the controller solution, such as linear convex combination theory, Cauchy's inequality and Jensen's inequality. To reduce the influence of larger time-delay on DETCS, we need to make a trade-off between network communication resource saving and network transmission time-delay, which can be realised by adjusting the event-triggered parameter in the event-triggered condition.

Remark 2: By combining the DETCS in data communication with the active fault-tolerant control method for nonlinear NCS, the fault/state information estimation and selection of the estimation information are realised in the intelligent sensor, and the fault accommodation and feedback control calculation are realised in the control unit. The intelligent sensor and the control unit can not only complete their respective functions and applications independently, but also communicate with each other and work together. All these form a distributed implementation architecture of estimation, selection, accommodation and control, which lays the foundation of the unified architecture for the subsequent integrated design between active fault tolerant control and network communication. This method can ensure the accuracy of fault estimation, the effective saving of network communication resources and the achievement of the system performance index.

C. DESIGN OF CONTINUOUS TIME STATE OBSERVER

According to Figure 1, we first need to design the observer at the front end of the event-generator. During a sampling period, the estimation of states and faults will be designed for sampled-data nonlinear NCSs (3) based on the mature theory method of the time-delay system [20]. Between two adjacent sampling instants, the input of the observer $y(i_k)$ and $u(i_k)$ can be converted to the corresponding $y(t-\tau_1(t))$ and $u(t-\tau_1(t))$ by converting the sampling period to time-delay $\tau_1(t)(t-\tau_1 = t-(t)i_k)$. Therefore, a continuous time-delay output can be obtained as follows:

$$y_i(t-\tau_1(t)) = \sum_{i=1}^{r} \mu_i(\theta(t))\boldsymbol{C}_i x(t-\tau_1(t)) \tag{5}$$

where $i_k \le t < i_{k+1}, 0 < \tau_1 \le h_\tau = h$.

We construct a continuous time state observer as follows:

$$\begin{cases} \bar{\hat{x}}_{(t)} = \sum_{i=1}^{r}\sum_{i=1}^{r} \mu_j(\theta(t))[\boldsymbol{A}_i\hat{x}(t) \\ \quad + \boldsymbol{B_i} sat(u(t-\tau_1(t))) + \boldsymbol{E}_{fi}\hat{f}(t) - \boldsymbol{L}_j(\hat{y}(t)-y(t))] \\ \hat{y}(t) = \sum_{i=1}^{r} \mu_i(\theta(t))[\boldsymbol{C}_i(\hat{x}(t)-\tau(t))] \end{cases} \tag{6}$$

where $\hat{x}(t)$, $\hat{y}(t)$ and $\hat{f}(t)$ d enote the estimation value of the state, the estimation value of the output and the estimation value of the fault, respectively. Define $e_x(t) = \hat{x}(t) - x(t)$, $e_y(t) = \hat{y}(t) - y(t)$, $e_f(t) = \hat{f}(t) - f(t)$, and $L_j \in R^{n\times m}$, $j = 1, 2, 3, \ldots, r$ is the filter to be designed.

D. ANALYSIS OF TRANSMISSION TIME-DELAY UNDER DETCS

After the event-generator, we get $\bigcup_{k=1}^{\infty}[t_k, t_{k+1}) = [0, \infty)$ for any transmission interval $[t_k, t_{k+1})$. h_k denotes the data transmission period in the back end of event-generator, and $h_k = t_{k+1} - t_k$. At the same time, the estimating data after the generator is transmitted in a non-uniform transmission period. Considering the effect of time-delay, when $u(\hat{t}_k)$ arrives at the holder and $u(\hat{t}_{k+1})$ does not arrive at the holder, we define a transmission interval as follows:

$$\Omega = [t_k + \tau_{t_k}, t_{k+1} + \tau_{t_{k+1}}) \tag{7}$$

The interval is divided into several sub-intervals:

$$\Omega = \Delta_k^0 \cup \cdots \Delta_k^{l_k} \cup \cdots \cup \Delta_k^{d_k} \tag{8}$$

where $\Delta_k^{l_k} = [t_k + l_k h + \tau_{t_k+l_k h}, t_k + (l_k+1)h + \tau_{t_{k+(l_k+1)h}})$; $l_k = 0, 1, 2, \cdots, d_k$; $d_k h = t_{k+1} - t_k - h$. We assume that $\tau_{t_k+l_k h}$ is the network transmission time-delay at the sample instant $t_{k+l_k h}$.

When $t \in \Delta_k^{l_k}$, we define the network transmission time-delay $\tau_2(t)$ as follows:

$$\tau_2(t) = t - t_k \tag{9}$$

In terms of (8) and (9), we can obtain the lower and upper bound of network transmission function $\tau_2(t)$:

$$\begin{aligned} 0 &< l_k h + \tau_{t_k+l_k h} \le \tau_2(t) \le (l_k+1)h + \tau_{t_{k+(l_k+1)h}} \\ &\le (d_k+1)h + \tau_{t_{k+(l_k+1)h}} = t_{k+1} - t_k + \tau_{t_{k+(l_k+1)h}} \le \bar{h} \\ &= h_{\max k} + \bar{\tau} \end{aligned} \tag{10}$$

where $\bar{h} = h_{\max k} + \bar{\tau} = h_{\max k} + \max\{\tau_{t_{k+(l_k+1)h}}\}$.

When $t \in \Delta_k^{l_k}$, we define the error $\hat{e}(i_k)$ between the state estimation value at the latest sample instant and the state estimation value at the latest transmission instant:

$$\hat{e}(i_k) = \hat{x}(i_k) - \hat{x}(t_k) \tag{11}$$

In terms of (11), the discrete event-triggered condition is obtained as follows:

$$\hat{e}^T(i_k)\Phi\hat{e}(i_k) \le \delta\hat{x}^T(t-\tau_2(t))\Phi\hat{x}(t-\tau_2(t)) \tag{12}$$

Remark 3: The smart sensor completes the estimation of state/fault and the selection of transmission data. There are two advantages to adopting the smart sensor. On the one hand, in the intelligent sensor, the fault information is estimated based on the sampler time-triggered at equal period (not event-triggered), which can ensure that the state/fault estimation information is more complete, accurate and timely. On the other hand, the calculation function of each agent in nonlinear NCSs is fully applied. The event-generator can select some transmission data from the sampling data, which releases the network transmission load and computing load of the controller CPU.

E. CLOSED-LOOP FAULT SYSTEM MODEL FOR NONLINEAR NCSs

Based on the faults and states information estimated in Part C, in Part E we will design an active fault-tolerant controller under non-uniform sampling. First, in order to adjust the system fault and achieve the performance index, we make the following assumption [17]:

$$rank(B_i, E_{fi}) = rank(B_i)$$

This assumption implies the existence of the matrix $\boldsymbol{B}_j^+ \in R^{n_u \times n}$, $j = 1, 2, 3, \cdots, r$ and $\boldsymbol{B}_j^+$ satisfies $(\boldsymbol{I} - \boldsymbol{B}_i\boldsymbol{B}_j^+)\boldsymbol{E}_{fi} = 0$. Furthermore, the existence of $\boldsymbol{B}_j^+$ can realise the accommodation of the system fault. Considering the effect of the time-delay and event-generator, the transmission data at the controller end are updated under the non-uniform mode. The non-uniform transmission state-feedback controller and time-varying fault accommodation fault-tolerant controller are proposed as follows:

$$u(t) = \sum_{i=1}^{r}\sum_{j=1}^{r}\mu_i(\theta(t))\mu_j(\theta(t))[-\boldsymbol{K}_j\hat{x}(t_k) - \boldsymbol{B}_j^+\boldsymbol{E}_{fi}\hat{f}(t_k)], \quad t \in [t_k, t_{k+1}) \tag{13}$$

where $\boldsymbol{K}_j \in R^{n_u \times n}, j = 1, 2, 3 \cdots r$ is the matrix gain of the controller to be designed.

In terms of (3), (7), and (13), we obtain

$$\begin{cases} \dot{x}(t) = \sum_{i=1}^{r}\sum_{j=1}^{r}\mu_i(\theta(t))\mu_j(\theta(t))[\boldsymbol{A}_i x(t) \\ \quad - \boldsymbol{B}_i sat(\boldsymbol{K}_j(\hat{x}(t-\tau_1(t)) - \hat{e}(t-\tau_1(t))) \\ \quad - \boldsymbol{B}_i sat(\boldsymbol{K}_j e_x(t-\tau_2(t)) - \boldsymbol{E}_{fi} e_f(t-\tau_2(t)) \\ \quad + \tau_2(t)\boldsymbol{E}_{fi}\dot{f}(t) + \boldsymbol{E}_{di}d(t)] \\ y(t) = \sum_{i=1}^{r}\mu_i(\theta(t))\boldsymbol{C}_i x(t_k) \end{cases} \tag{14}$$

Remark 4: The closed-loop fault system model (14) integrates many factors into one framework, such as network attributes, actuator saturation constraints, fault estimation, disturbance information, and event-triggered information. The establishment of the closed-loop fault system model lays solid foundations for cooperation to solve the state-feedback controller gain $\boldsymbol{K}_j$, the fault accommodator gain $\boldsymbol{B}_j^+$, and the event-triggered weight matrix gain $\boldsymbol{\Phi}$. Namely, its establishment ensures that the integrated design combining active fault-tolerant control and communication becomes possible.

III. ESTIMATION OF TIME-VARYING FAULT AND STATE

Based on (6) and the related definitions, the error system is

$$\begin{cases} \dot{e}_x(t) = \sum_{i=1}^{r}\sum_{j=1}^{r}\mu_i(\theta(t))\mu_j(\theta(t))[\boldsymbol{A}_i e_x(t) + \boldsymbol{E}_{fi} e_f(t) \\ \quad - \boldsymbol{E}_{di}d(t) - \boldsymbol{L}_j\boldsymbol{C}_i e_x(t-\tau_1(t)) + \boldsymbol{L}_j\boldsymbol{D}_{vi}v(t-\tau_1(t))] \\ e_y(t) = \sum_{i=1}^{r}\mu_i(\theta(t))[\boldsymbol{C}_i e_x(t-\tau_1(t)) - \boldsymbol{D}_{vi}v(t-\tau_1(t))] \end{cases} \tag{15}$$

We extend $e_x(t)$ and $e_f(t)$ into a whole entity to estimate the continuous time-varying fault conveniently. We adopt the fault estimation algorithm as follows:

$$\dot{\hat{f}}(t) = -\sum_{j=1}^{r}\mu_j(\theta(t))\boldsymbol{F}_j e_y(t) \tag{16}$$

where $F_j \in R^{n \times m}, j = 1, 2, 3 \cdots r$ is the state estimation matrix to be designed.

According to (16), the time derivative of fault estimation error can be written as

$$\dot{e}_f(t) = \sum_{i=1}^{r}\sum_{j=1}^{r}\mu_i(\theta(t))\mu_j(\theta(t))[-\boldsymbol{F}_j\boldsymbol{C}_i e_x(t-\tau_1(t)) + \boldsymbol{F}_j\boldsymbol{D}_{vi}v(t-\tau_1(t)) - \dot{f}(t)] \tag{17}$$

Then the augmented model of state estimation error and fault estimation error is

$$\dot{\overline{e}}(t) = \sum_{i=1}^{r}\sum_{j=1}^{r}\mu_i(\theta(t))\mu_j(\theta(t))[\boldsymbol{P}\overline{\boldsymbol{A}}_i\overline{e}(t) - \overline{\boldsymbol{L}}_j\overline{\boldsymbol{C}}_i\overline{e}(t-\tau_1(t)) + \overline{\boldsymbol{E}}_{di}d(t) + \overline{\boldsymbol{L}}_j\boldsymbol{D}_{vi}v(t-\tau_1(t))] \tag{18}$$

where $\overline{e}(t) = \begin{bmatrix} e_x(t) \\ e_f(t) \end{bmatrix}$ $\overline{d}(t) = \begin{bmatrix} d(t) \\ \dot{f}(t) \end{bmatrix}$, $\boldsymbol{P}\overline{\boldsymbol{A}}_i = \begin{bmatrix} \boldsymbol{A}_i & \boldsymbol{E}_{fi} \\ 0 & 0 \end{bmatrix}$, $\overline{\boldsymbol{E}}_{di} = \begin{bmatrix} \boldsymbol{E}_{di} & 0 \\ 0 & \boldsymbol{I} \end{bmatrix}$, $\overline{\boldsymbol{L}}_j = \begin{bmatrix} \boldsymbol{L}_j \\ \boldsymbol{F}_j \end{bmatrix}$, $\overline{\boldsymbol{C}}_i = [\boldsymbol{C}_i \ 0]$.

The design goal of fault estimation and state estimation is that, according to the sampling data of nonlinear NCSs (3), we seek the matrix gain of robust observer $\overline{\boldsymbol{L}}_j$, which satisfies the following conditions. The system (18) is asymptotically stable; The disturbance $d(t)$ and the measurement noise satisfy the optimal H_∞-performance index $\|\overline{e}(t)\|_2^2 \le \gamma_1^2(\|d(t)\|_2^2 + \sum_{k=0}^{\infty}(i_{k+1} - i_k)\|v(i_k)\|_2^2)$.

Theorem 1: For the sampling data of nonlinear NCSs (3), we adopt the continuous time state observer (6) and fault estimator (16). If there exist positive definite matrices $\boldsymbol{P} > 0, \boldsymbol{Q} > 0, \boldsymbol{S} > 0, \boldsymbol{R} > 0, \boldsymbol{N}$, and $\boldsymbol{Z}$, which satisfy

$$\min \gamma_1 \quad \text{s.t. } (19) \sim (20)$$

$$\begin{bmatrix} \Xi_{11}^{(1)} & \Xi_{12}^{(1)} & \Xi_{13}^{(1)} & \Xi_{14}^{(1)} & 0 \\ * & \Xi_{22}^{(1)} & \Xi_{23}^{(1)} & \Xi_{24}^{(1)} & \Xi_{25}^{(1)} \\ * & * & \Xi_{33}^{(1)} & \Xi_{34}^{(1)} & 0 \\ * & * & * & -\gamma_1^2 \boldsymbol{I} & \Xi_{45}^{(1)} \\ * & * & * & * & -h_\tau n_1 \boldsymbol{P} \end{bmatrix} < \boldsymbol{0} \tag{19-a}$$

$$\begin{bmatrix} \Xi_{11}^{(2)} & \Xi_{12}^{(2)} & \boldsymbol{P}\overline{\boldsymbol{E}}_{di} & \boldsymbol{Y}\boldsymbol{D}_{vi} \\ * & \Xi_{22}^{(2)} & 0 & 0 \\ * & * & -\gamma_1^2 \boldsymbol{I} & 0 \\ * & * & * & -\gamma_1^2 \boldsymbol{I} \end{bmatrix} < \boldsymbol{0} \tag{19-b}$$

$$\begin{bmatrix} \boldsymbol{R} & \boldsymbol{N}^T \\ * & \boldsymbol{Z} \end{bmatrix} > 0 \tag{20}$$

then the augmented system (18) is asymptotically stable, that is, the state estimation error $e_x(t)$ and time-varying fault estimation error $e_f(t)$ are asymptotically stable, and satisfy the optimal H_∞-performance index $\|\bar{e}(t)\|_2^2 \leq \gamma_1^2(\|d(t)\|_2^2 + \sum_{k=0}^{\infty}(i_{k+1} - i_k)\|v(i_k)\|_2^2)$

where

$$\begin{aligned}
\Xi_{11}^{(1)} &= \boldsymbol{P}\overline{\boldsymbol{A}}_i + \boldsymbol{P}\overline{\boldsymbol{A}}_i^T\boldsymbol{P} - n_2\boldsymbol{P} + \boldsymbol{I} + \boldsymbol{N}_1 + \boldsymbol{N}_1^T \\
&\quad + h_\tau n_1 \boldsymbol{P}\overline{\boldsymbol{A}}_i^T\boldsymbol{P}\overline{\boldsymbol{A}}_i + h_\tau n_2(\boldsymbol{P}\overline{\boldsymbol{A}}_i + \boldsymbol{P}\overline{\boldsymbol{A}}_i^T\boldsymbol{P}), \\
\Xi_{12}^{(1)} &= -\boldsymbol{Y}_j\overline{\boldsymbol{C}}_i + n_2\boldsymbol{P} - \boldsymbol{N}_1 + \boldsymbol{N}_2^T - h_\tau n_1 \boldsymbol{P}\overline{\boldsymbol{A}}_i^T\boldsymbol{Y}_j\overline{\boldsymbol{C}}_i \\
&\quad - h_\tau n_2 \boldsymbol{Y}_j\overline{\boldsymbol{C}}_i - h_\tau n_2 \boldsymbol{P}\overline{\boldsymbol{A}}_i^T\boldsymbol{P}, \\
\Xi_{13}^{(1)} &= \boldsymbol{P}\overline{\boldsymbol{E}}_{di} + h_\tau n_1 \boldsymbol{P}\overline{\boldsymbol{A}}_i^T\boldsymbol{P}\overline{\boldsymbol{E}}_{di} + h_\tau n_2 \boldsymbol{P}\overline{\boldsymbol{E}}_{di}, \\
\Xi_{14}^{(1)} &= \boldsymbol{Y}_j\boldsymbol{D}_{vi} + h_\tau n_1 \boldsymbol{P}\overline{\boldsymbol{A}}_i^T\boldsymbol{Y}_j\boldsymbol{D}_{vi} + h_\tau n_2 \boldsymbol{Y}_j\boldsymbol{D}_{vi}, \\
\Xi_{22}^{(1)} &= -h_\tau n_3\boldsymbol{P} - n_2\boldsymbol{P} - \boldsymbol{N}_2 - \boldsymbol{N}_2^T + h_\tau n_2 \boldsymbol{Y}_j\overline{\boldsymbol{C}}_i \\
&\quad + h_\tau n_2 \overline{\boldsymbol{C}}_i^T\boldsymbol{Y}_j^T + 2n_3h_\tau\boldsymbol{P}, \\
\Xi_{23}^{(1)} &= -h_\tau n_1 \overline{\boldsymbol{C}}_i^T\boldsymbol{Y}^T\overline{\boldsymbol{E}}_{di}^T - h_\tau n_2 \boldsymbol{P}\overline{\boldsymbol{E}}_{di}, \\
\Xi_{24}^{(1)} &= -h_\tau n_2 \boldsymbol{Y}_j\boldsymbol{D}_{vi},\ \Xi_{25}^{(1)} = h_\tau n_1 \overline{\boldsymbol{C}}_i^T\boldsymbol{Y}_j^T, \\
\Xi_{33}^{(1)} &= h_\tau n_1 \overline{\boldsymbol{E}}_{di}^T\boldsymbol{P}\overline{\boldsymbol{E}}_{di} - \gamma_1^2\boldsymbol{I},\ \Xi_{34}^{(1)} = h_\tau n_1 \overline{\boldsymbol{E}}_{di}^T\boldsymbol{Y}_j\boldsymbol{D}_{vi}, \\
\Xi_{45}^{(1)} &= -h_\tau n_1 \boldsymbol{D}_{vi}^T\boldsymbol{Y}_i^T, \\
\Xi_{11}^{(2)} &= \boldsymbol{P}\overline{\boldsymbol{A}}_i + \boldsymbol{P}\overline{\boldsymbol{A}}_i^T\boldsymbol{P} - n_2\boldsymbol{P} + \boldsymbol{I} + \boldsymbol{N}_1 + \boldsymbol{N}_1^T - h_\tau\boldsymbol{Z}_1, \\
\Xi_{12}^{(2)} &= -\boldsymbol{P}\overline{\boldsymbol{C}} + n_2\boldsymbol{P} - \boldsymbol{N}_1 + \boldsymbol{N}_2^T + h_\tau\boldsymbol{Z}_2, \\
\Xi_{22}^{(2)} &= -h_\tau n_3\boldsymbol{P} - n_2\boldsymbol{P} - \boldsymbol{N}_2 - \boldsymbol{N}_2^T - h_\tau\boldsymbol{Z}_3
\end{aligned}$$

Proof: Firstly, we construct a Lyapunov-functional candidate as follows:

$$\begin{aligned}
V(t) &= \bar{e}^T(t)\boldsymbol{P}\bar{e}(t) \\
&\quad + (h_\tau - \tau_1(t))\tau_1(t)\bar{e}^T(t - \tau_1(t))\boldsymbol{Q}\bar{e}(t - \tau_1(t)) \\
&\quad + (h_\tau - \tau_1(t))\int_{i_k}^{t} \dot{\bar{e}}^T(s)\boldsymbol{R}\dot{\bar{e}}(s)ds \\
&\quad + (h_\tau - \tau_1(t))\vartheta^T(t)\boldsymbol{S}\vartheta(t)
\end{aligned} \tag{21}$$

where $\boldsymbol{P} = \boldsymbol{P}^T > 0, \boldsymbol{Q} = \boldsymbol{Q}^T > 0, \boldsymbol{R} = \boldsymbol{R}^T > 0, \boldsymbol{S} = \boldsymbol{S}^T > 0$, and $\vartheta(t) = \bar{e}(t) - \bar{e}(i_k)$.

Along with (18), the time derivative of the Lyapunov-functional candidate is obtained as follows:

$$\begin{aligned}
\dot{V}(t) &= 2\bar{e}^T(t)\boldsymbol{P}\dot{\bar{e}}(t) - h_\tau\bar{e}^T(t - \tau_1(t))\boldsymbol{Q}\bar{e}(t - \tau_1(t)) \\
&\quad + 2(h_\tau - \tau_1(t))\bar{e}^T(t - \tau_1(t))\boldsymbol{Q}\bar{e}(t - \tau_1(t)) \\
&\quad + 2(h_\tau - \tau_1(t))\vartheta^T(t)\boldsymbol{S}\dot{\bar{e}}(t) \\
&\quad + (h_\tau - \tau_1(t))\dot{\bar{e}}^T(t)\boldsymbol{R}\dot{\bar{e}}(t) - \vartheta^T(t)\boldsymbol{S}\vartheta(t) \\
&\quad - \int_{i_k}^{t} \dot{\bar{e}}^T(s)\boldsymbol{R}\dot{\bar{e}}(s)ds
\end{aligned} \tag{22}$$

We set $\overline{d}(t) = 0, v(i_k) = 0$ to ensure that the error system has asymptotic stability.

We define $\xi(t) = [\bar{e}^T(t), \bar{e}^T(i_k)]^T$ to deal with the integral term in (22). For arbitrary matrix $\boldsymbol{N} \in R^{2(n+n_f)\times(n+n_f)}$, we get (23) based on the Cauchy inequality, Jensen inequality, and the properties of the Schur complement lemma.

$$-\int_{i_k}^{t} \dot{\bar{e}}^T(s)\boldsymbol{R}\dot{\bar{e}}(s)ds \leq 2\xi^T(t)\boldsymbol{N}\vartheta(t) + \tau_1(t)\xi^T(t)\boldsymbol{Z}\xi(t) \tag{23}$$

where $\boldsymbol{R}$, $\boldsymbol{N}$,and $\boldsymbol{Z}$ satisfy (20).

Plugging (23) into (22), we obtain

$$\begin{aligned}
\dot{V}(t) &\leq 2\bar{e}^T(t)\boldsymbol{P}\dot{\bar{e}}(t) - h_\tau\bar{e}^T(t - \tau_1(t))\boldsymbol{Q}\bar{e}(t - \tau_1(t)) \\
&\quad + 2(h_\tau - \tau_1(t))\bar{e}^T(t - \tau_1(t))\boldsymbol{Q}\bar{e}(t - \tau_1(t)) \\
&\quad + 2(h_\tau - \tau_1(t))\vartheta^T(t)\boldsymbol{S}\dot{\bar{e}}(t) \\
&\quad + (h_\tau - \tau_1(t))\dot{\bar{e}}^T(t)\boldsymbol{R}\dot{\bar{e}}(t) - \vartheta^T(t)\boldsymbol{S}\vartheta(t) \\
&\quad + 2\xi^T(t)\boldsymbol{N}\vartheta(t) + \tau_1(t)\xi^T(t)\boldsymbol{Z}\xi(t) \\
&= \xi^T(t)[\boldsymbol{\Gamma}_1 + (h_\tau - \tau_1(t))\boldsymbol{\Gamma}_2 + \tau_1(t)\boldsymbol{Z}]\xi(t)
\end{aligned} \tag{24}$$

where $\bar{e}(t) = \boldsymbol{M}_1\xi(t), \vartheta(t) = \boldsymbol{M}_2\xi(t), \dot{\bar{e}}(t) = \boldsymbol{M}_3\xi(t), \bar{e}(r_k) = \boldsymbol{M}_4\xi(t), \boldsymbol{M}_1 = [\boldsymbol{I}\ 0], \boldsymbol{M}_2 = [\boldsymbol{I}\ -\boldsymbol{I}], \boldsymbol{M}_3 = [\boldsymbol{P}\overline{\boldsymbol{A}}_i - \overline{\boldsymbol{L}}_j\overline{\boldsymbol{C}}_i], \boldsymbol{M}_4 = [0\ \boldsymbol{I}], \boldsymbol{\Gamma}_1 = 2\boldsymbol{M}_1^T\boldsymbol{P}\boldsymbol{M}_3 - h_\tau\boldsymbol{M}_4^T\boldsymbol{Q}\boldsymbol{M}_4 - \boldsymbol{M}_2^T\boldsymbol{S}\boldsymbol{M}_2 + 2\boldsymbol{N}\boldsymbol{M}_2, \boldsymbol{\Gamma}_2 = 2\boldsymbol{M}_4^T\boldsymbol{Q}\boldsymbol{M}_4 + 2\boldsymbol{M}_2^T\boldsymbol{S}\boldsymbol{M}_3 + \boldsymbol{M}_3^T\boldsymbol{R}\boldsymbol{M}_3$.

In terms of Lemma 3 in [22], $\dot{V}(t) < 0$ is equivalent to

$$\boldsymbol{\Gamma}_1 + h_\tau\boldsymbol{\Gamma}_2 < 0, \quad \boldsymbol{\Gamma}_1 + h_\tau\boldsymbol{Z} < 0 \tag{25}$$

When $\overline{d}(t) \neq 0, v(i_k) \neq 0$, we consider the following H_∞ performance index function under the zero initial condition:

$$\begin{aligned}
J = \dot{V}(t) + \bar{e}^T(t)\bar{e}(t) - \gamma_1^2(\overline{d}^T(t)\overline{d}(t) \\
+ v^T(i_k)v(i_k)) < 0
\end{aligned} \tag{26}$$

Substituting $\dot{V}(t)$ of (24) into (26), we get

$$\boldsymbol{\Gamma}_1' + (h_\tau - \tau_1(t))\boldsymbol{\Gamma}_2' + \tau_1(t)\begin{bmatrix} \boldsymbol{Z} & 0 & 0 \\ 0 & 0 & 0 \\ 0 & 0 & 0 \end{bmatrix} < 0 \tag{27}$$

where $\zeta^T(t) = [\bar{e}^T(t)\ \bar{e}^T(i_k)\ \overline{d}^T(t)\ v^T(i_k)], \xi(t) = \boldsymbol{M}_4'\zeta(t), [\overline{d}^T(t)\ v^T(i_k)] = \boldsymbol{M}_5'\zeta(t), \bar{e}(i_k) = \boldsymbol{M}_6'\zeta(t), \boldsymbol{M}_1' = [\boldsymbol{I}\ \boldsymbol{0}\ \boldsymbol{0}\ \boldsymbol{0}], \boldsymbol{M}_2' = [\boldsymbol{I}\ -\boldsymbol{I}\ \boldsymbol{0}\ \boldsymbol{0}], \boldsymbol{M}_3' = [\overline{\boldsymbol{A}}_i\ -\overline{\boldsymbol{L}}_j\overline{\boldsymbol{C}}_i\ \overline{\boldsymbol{E}}_{di}\ \overline{\boldsymbol{L}}_j\boldsymbol{D}_{vi}], \boldsymbol{M}_4' = [\boldsymbol{I}\ \boldsymbol{I}\ \boldsymbol{0}\ \boldsymbol{0}], \boldsymbol{M}_5' = [\boldsymbol{0}\ \boldsymbol{0}\ \boldsymbol{I}\ \boldsymbol{I}], \boldsymbol{M}_6' = [\boldsymbol{0}\ \boldsymbol{I}\ \boldsymbol{0}\ \boldsymbol{0}], \boldsymbol{\Gamma}_1' = 2\boldsymbol{M}_1'^T\boldsymbol{P}\boldsymbol{M}_3' - h_\tau\boldsymbol{M}_6'^T\boldsymbol{Q}\boldsymbol{M}_6' - \boldsymbol{M}_2'^T\boldsymbol{S}\boldsymbol{M}_2' + 2[\boldsymbol{N}^T\ \boldsymbol{0}\ \boldsymbol{0}]^T\boldsymbol{M}_2, \boldsymbol{\Gamma}_2' = 2\boldsymbol{M}_6'^T\boldsymbol{Q}\boldsymbol{M}_6' + 2\boldsymbol{M}_2'^T\boldsymbol{S}\boldsymbol{M}_3' + \boldsymbol{M}_3'^T\boldsymbol{R}\boldsymbol{M}_3'$.

Similarly, (27) is equivalent to (28) by applying Lemma 3 of [22] again.

$$\mathbf{\Gamma}_1' + h_\tau \mathbf{\Gamma}_2' < 0, \quad \mathbf{\Gamma}_1' + h_\tau \begin{bmatrix} \mathbf{Z} & 0 & 0 \\ 0 & 0 & 0 \\ 0 & 0 & 0 \end{bmatrix} < 0 \quad (28)$$

Furthermore, we assume that $\boldsymbol{R} = n_1\boldsymbol{P}$, $\boldsymbol{S} = n_2\boldsymbol{P}$, $\boldsymbol{Q} = n_3\boldsymbol{P}$, $\boldsymbol{P}\overline{\boldsymbol{L}}_j = \boldsymbol{Y}_j(\overline{\boldsymbol{L}}_j = \boldsymbol{P}^{-1}\boldsymbol{Y}_j)$ to transfer the nonlinear matrix inequality into the corresponding linear matrix inequality conveniently. Plugging them into (28), we get

$$\mathbf{\Gamma}_1'' + h_\tau \mathbf{\Gamma}_2'' < 0, \quad \mathbf{\Gamma}_1'' + h_\tau \begin{bmatrix} \mathbf{Z} & 0 & 0 \\ 0 & 0 & 0 \\ 0 & 0 & 0 \end{bmatrix} < 0 \quad (29)$$

With limited space, we have omitted the relevant expressions of $\mathbf{\Gamma}_1''$ and $\mathbf{\Gamma}_2''$.

Equation (29) is equivalent to (19) in Theorem 1 by adopting the Schur complement lemma. If (19) is satisfied, the state estimation error e_x and fault estimation error e_f show asymptotic convergence.

From 0 to ∞, we get (30) by integrating for (26).

$$\begin{aligned} V(+\infty) - V(0) \leq &- \int_0^{+\infty} (\overline{e}^T(s)\overline{e}(s))\mathrm{d}s \\ &+ \gamma_1^2 \int_0^{+\infty} (d^T(s)d(s))\mathrm{d}s \\ &+ \gamma_1^2 \sum_{k=0}^{+\infty} (i_{k+1} - i_k)(v^T(i_k)v(i_k)) \end{aligned} \quad (30)$$

where $d(t) \in L_2[0, +\infty)$, $v(i_k) \in L_2[0, +\infty)$. Under the zero initial condition, there are $V(0) = 0$ and $V(+\infty) \geq 0$. Then (30) is equivalent to

$$\begin{aligned} \int_0^{+\infty} \overline{e}^T(s)\overline{e}(s)\mathrm{d}s \leq \gamma_1^2 &\int_0^{+\infty} (d^T(s)d(s))\mathrm{d}s \\ &+ \gamma_1^2 \sum_{k=0}^{+\infty} (i_{k+1} - i_k)(v^T(i_k)v(i_k)) \end{aligned} \quad (31)$$

That is, $\left\|\overline{e}^T(t)\right\|_2^2 \leq \gamma_1^2(\left\|\overline{d}^T(t)\right\|_2^2 + \sum_{k=0}^{+\infty}(i_{k+1}-i_k)\left\|v(i_k)\right\|_2^2)$, and the related H_∞-performance index is satisfied. The proof process is completed.

Remark 5: Theorem 1 adds one item $(h_\tau - \tau_1(t))\tau_1(t)\,\overline{e}^T(t-\tau_1(t))\boldsymbol{Q}\overline{e}(t-\tau_1(t))$ into the Lyapunov function concerned by comparing with [17], which reduces the conservatism of the results. The estimation error of the continuous time-varying fault and state will possess smaller error compared with [17].

IV. INTEGRATED DESIGN METHOD BETWEEN FAULT-ACCOMMODATION AND COMMUNICATION

In terms of Theorem 1, the state estimation error $e_x(t_k)$ and the fault estimation error $e_f(t_k)$ remain asymptotically stable and satisfy the H_∞-performance index by adopting the continuous time observer. However, there are dynamic and static errors which will be bound to influence the fault-tolerant performance. Therefore, we consider $e_x(t_k)$ and $e_f(t_k)$ as a kind of external disturbance when we design the fault-tolerant controller. Furthermore, the active fault-tolerant controller possesses robust performance for these disturbances by adopting the design idea of H_∞. Similarly, we can also treat $\tau_2(t)\boldsymbol{E}_{fi}\dot{f}(t)$ as another kind of disturbance. According to the results of the state estimation and continuous time-varying fault estimation in Theorem 1, the following theorem is proposed by adopting the state feedback and fault accommodation fault-tolerant controller (13) under non-uniform transmission.

The goal of the satisfactory integrated design of fault accommodation and communication is as follows: considering the effects of non-uniform transmission and actuator saturation, we seek the state feedback gain matrix $\boldsymbol{K}_j$, fault accommodation matrix $\boldsymbol{B}_j^+$, and event-triggered weight matrix $\mathbf{\Phi}$ under DETCS. They ensure that the closed-loop fault nonlinear NCSs possess α-stability, the general $\boldsymbol{H}_\infty/\boldsymbol{H}_2$-performance index and as little as possible network communication.

Theorem 2: For the non-uniform transmission nonlinear NCSs (14) which are derived from the sampling data nonlinear NCSs (3), we set $\overline{h}$, Υ_i, Υ_i^-, α, $\tilde{\gamma}_1$, $\tilde{\gamma}_2$ in advance. If there exist some positive definite matrices $\tilde{\boldsymbol{P}} > 0, \tilde{\boldsymbol{S}} > 0, \tilde{\boldsymbol{Q}} > 0, \tilde{\boldsymbol{R}} > 0$, and some matrices with appropriate dimensions $\tilde{\boldsymbol{N}}'$, $\tilde{\boldsymbol{Z}}'$, $\boldsymbol{Q}_1, \boldsymbol{Q}_2, \boldsymbol{Q}_3, \boldsymbol{Q}_4, \boldsymbol{Q}_5, \boldsymbol{Q}_6$, which satisfy the following linear matrix inequality

$$\begin{bmatrix} \tilde{\mathbf{\Xi}}^{(1)} & 0 & 0 & \tilde{\Psi}^{(1)} \\ * & -\mathbf{\Phi} & 0 & 0 \\ * & * & -\delta\mathbf{\Phi} & 0 \\ * & * & * & -\frac{\overline{h}^2}{4}m_3\tilde{\boldsymbol{P}} - \overline{h}n_2\tilde{\boldsymbol{P}} \end{bmatrix} < 0 \quad \text{(32-a)}$$

$$\begin{bmatrix} \hat{\mathbf{\Xi}}^{(1)} & 0 & 0 & \hat{\Psi}^{(1)} \\ * & -\mathbf{\Phi} & 0 & 0 \\ * & * & -\delta\mathbf{\Phi} & 0 \\ * & * & * & -\frac{\overline{h}^2}{4}m_3\tilde{\boldsymbol{P}} \end{bmatrix} < 0 \quad \text{(32-b)}$$

$$\begin{bmatrix} \tilde{\boldsymbol{P}} & \boldsymbol{C}_i^T \\ * & \tilde{\boldsymbol{Z}}' \end{bmatrix} > 0, \quad \begin{bmatrix} \boldsymbol{Q}_1 & \boldsymbol{E}_{fi}^T\tilde{\boldsymbol{P}} \\ * & \boldsymbol{Q}_2 \end{bmatrix} > 0,$$

$$\begin{bmatrix} \boldsymbol{Q}_3 & \boldsymbol{E}_{fi}^T\tilde{\boldsymbol{S}} \\ * & \boldsymbol{Q}_4 \end{bmatrix} > 0, \quad \begin{bmatrix} \boldsymbol{Q}_5 & \boldsymbol{E}_{fi}^T\tilde{\boldsymbol{R}} \\ * & \boldsymbol{Q}_6 \end{bmatrix} > 0 \quad \text{(32-c, d, e, f)}$$

$$\begin{bmatrix} \tilde{\boldsymbol{P}} & \boldsymbol{C}_i^T \\ * & \tilde{\gamma}_2^2\boldsymbol{I} \end{bmatrix} \geq 0 \quad (33)$$

$$\begin{bmatrix} 1 & \overline{f}_{\tilde{l}} \\ * & \tilde{\boldsymbol{P}}^{-1} \end{bmatrix} > 0, \quad \text{for } \tilde{l} \in [1, m] \quad (34)$$

then the non-uniform transmission active fault-tolerant controller (13) can ensure that the closed-loop fault system (14) with continuous time-varying fault possesses α-stability, and the generalised H_∞/H_2 performance in attraction domain $\varepsilon(\boldsymbol{P})$. The related indices are $\|\eta(t)\|_2^2 \leq \tilde{\gamma}_1^2\|d_\alpha(t)\|_2^2 + \tilde{\gamma}_1^2 \sum_{k=0}^{\infty}(t_{k+1} - t_k)(\left\|e_\eta(t_k)\right\|_2^2 + \left\|e_{f_\alpha}(t_k)\right\|_2^2)$, $\|y_\alpha(t)\|_\infty \leq \tilde{\gamma}_2\|d_\alpha(t)\|_2 + \tilde{\gamma}_2 \sum_{k=0}^{\infty}(t_{k+1} - t_k)(\left\|e_\eta(t_k)\right\|_2 + \left\|e_{f_\alpha}(t_k)\right\|_2 + \|v(t_k)\|_2)$. Furthermore, we can obtain the satisfactory fault-tolerant controller $\boldsymbol{K}_j = (\tilde{\boldsymbol{P}}\tilde{\boldsymbol{B}}_i)^{-1}\overline{\boldsymbol{K}}_j$ and event-triggered weight matrix $\mathbf{\Phi}$, where

$$\begin{aligned}
\tilde{\Xi}_{11}^{(1)} &= \mathbf{\Lambda}_1 + \bar{h}n_2(\boldsymbol{A}_i+\alpha\boldsymbol{I})^{\mathrm{T}}\tilde{\boldsymbol{P}}(\boldsymbol{A}_i+\alpha\boldsymbol{I}) \\
&\quad + \bar{h}n_1\tilde{\boldsymbol{P}}(\boldsymbol{A}_i+\alpha\boldsymbol{I}) + \bar{h}n_1(\boldsymbol{A}_i+\alpha\boldsymbol{I})^{\mathrm{T}}\tilde{\boldsymbol{P}}, \\
\tilde{\Xi}_{12}^{(1)} &= \mathbf{\Lambda}_2 - \bar{h}n_1(\boldsymbol{A}_i+\alpha\boldsymbol{I})^{\mathrm{T}}\tilde{\boldsymbol{P}} \\
&\quad - \bar{h}n_2 exp(\alpha\tau_2(t))(\boldsymbol{A}_i+\alpha\boldsymbol{I})^T\{\Upsilon_q\overline{\boldsymbol{K}}_j+\Upsilon_q^-\overline{\boldsymbol{F}}_j\} \\
&\quad - \bar{h}n_2 exp(\alpha\tau_2(t))\{\Upsilon_q\overline{\boldsymbol{K}}_j+\Upsilon_q^-\overline{\boldsymbol{F}}_j\}, \\
\tilde{\Xi}_{13}^{(1)} &= \mathbf{\Lambda}_3 - \bar{h}n_2 exp(\alpha\tau_2(t))(\boldsymbol{A}_i+\alpha\boldsymbol{I})^T\{\Upsilon_q\overline{\boldsymbol{K}}_j+\Upsilon_q^-\overline{\boldsymbol{F}}_j\} \\
&\quad - \bar{h}n_1 exp(\alpha\tau_2(t))\{\Upsilon_q\overline{\boldsymbol{K}}_j+\Upsilon_q^-\overline{\boldsymbol{F}}_j\}, \\
\tilde{\Xi}_{14}^{(1)} &= \mathbf{\Lambda}_4 - \bar{h}n_2 exp(\alpha\tau_2(t))(\boldsymbol{A}_i+\alpha\boldsymbol{I})^T\tilde{\boldsymbol{P}}\boldsymbol{E}_{fi} \\
&\quad - \bar{h}n_1 exp(\alpha\tau_2(t))\tilde{\boldsymbol{P}}\boldsymbol{E}_{fi}, \\
\tilde{\mathbf{\Pi}}_{15}^{(1)} &= \mathbf{\Lambda}_5 + \bar{h}n_2(\boldsymbol{A}+\alpha\boldsymbol{I})^T\tilde{\boldsymbol{P}}\boldsymbol{E}_d + \bar{h}n_1\tilde{\boldsymbol{P}}\boldsymbol{E}_d, \\
\tilde{\Xi}_{22}^{(1)} &= \mathbf{\Lambda}_6 + \bar{h}n_3\tilde{\boldsymbol{P}} + \bar{h}n_1 exp(\alpha\tau_2(t))\{\Upsilon_q\overline{\boldsymbol{K}}_j+\Upsilon_q^-\overline{\boldsymbol{F}}_j\} \\
&\quad + \bar{h}n_1 exp(\alpha\tau_2(t))\{\Upsilon_q\overline{\boldsymbol{K}}_j^T+\Upsilon_q^-\overline{\boldsymbol{F}}_j^T\}, \\
\tilde{\Xi}_{23}^{(1)} &= \bar{h}n_1 exp(\alpha\tau_2(t))\{\Upsilon_q\overline{\boldsymbol{K}}_j+\Upsilon_q^-\overline{\boldsymbol{F}}_j\}, \\
\tilde{\Xi}_{24}^{(1)} &= \mathbf{\Lambda}_7 + \bar{h}n_2 exp(2\alpha\tau_2(t))\{\Upsilon_q\overline{\boldsymbol{K}}_j^T+\Upsilon_q^-\overline{\boldsymbol{F}}_j^T\}\boldsymbol{E}_{fi} \\
&\quad + \bar{h}n_1 exp(\alpha\tau_2(t))\tilde{\boldsymbol{P}}\boldsymbol{E}_{fi}, \\
\tilde{\Xi}_{25}^{(1)} &= \mathbf{\Lambda}_8 - \bar{h}n_2 exp(\alpha\tau_2(t))\{\Upsilon_q\overline{\boldsymbol{K}}_j^T+\Upsilon_q^-\overline{\boldsymbol{F}}_j^T\}\boldsymbol{E}_{di} \\
&\quad - \bar{h}n_1\tilde{\boldsymbol{P}}\boldsymbol{E}_{di}, \\
\tilde{\Xi}_{34}^{(1)} &= \mathbf{\Lambda}_{10} + \bar{h}n_2 exp(2\alpha\tau_2(t))\{\Upsilon_q\overline{\boldsymbol{K}}_j^T+\Upsilon_q^-\overline{\boldsymbol{F}}_j^T\}\boldsymbol{E}_{fi}, \\
\tilde{\Xi}_{35}^{(1)} &= \mathbf{\Lambda}_{11} - \bar{h}n_2 exp(\alpha\tau_2(t))\{\Upsilon_q\overline{\boldsymbol{K}}_j^T+\Upsilon_q^-\overline{\boldsymbol{F}}_j^T\}\boldsymbol{E}_{di}, \\
\tilde{\Xi}_{44}^{(1)} &= \mathbf{\Lambda}_{13} - \bar{h}n_2 exp(2\alpha\tau_2(t))\boldsymbol{E}_{fi}^T\tilde{\boldsymbol{P}}\boldsymbol{E}_{fi}, \\
\tilde{\Xi}_{45}^{(1)} &= \mathbf{\Lambda}_{14} - \bar{h}n_2 exp(\alpha\tau_2(t))\boldsymbol{E}_{fi}^T\tilde{\boldsymbol{P}}\boldsymbol{E}_{di}, \\
\tilde{\Xi}_{55}^{(1)} &= \mathbf{\Lambda}_{15} + \bar{h}n_2\boldsymbol{E}_{di}^T\tilde{\boldsymbol{P}}\boldsymbol{E}_{di}, \\
\tilde{\mathbf{\Psi}}_{21}^{(1)} &= \mathbf{\Lambda}_9 + \bar{h}n_2 exp(\alpha\tau_2(t))\{\Upsilon_q\overline{\boldsymbol{K}}_j^T+\Upsilon_q^-\overline{\boldsymbol{F}}_j^T\}, \\
\tilde{\mathbf{\Psi}}_{31}^{(1)} &= \mathbf{\Lambda}_{12} + \bar{h}n_2 exp(\alpha\tau_2(t))\{\Upsilon_q\boldsymbol{K}_j^T+\Upsilon_q^-\overline{\boldsymbol{F}}_j^T\}, \\
\hat{\Xi}_{11}^{(1)} &= \mathbf{\Lambda}_1 + \bar{h}\boldsymbol{Z}_1 + \bar{h}m_1\tilde{\boldsymbol{P}},\ \hat{\Xi}_{12}^{(1)} = \mathbf{\Lambda}_2 - h\boldsymbol{Z}_2 \\
\hat{\Xi}_{13}^{(1)} &= \mathbf{\Lambda}_3,\ \hat{\Xi}_{14}^{(1)} = \mathbf{\Lambda}_4,\ \hat{\Xi}_{15}^{(1)} = \mathbf{\Lambda}_5, \\
\hat{\Xi}_{22}^{(1)} &= \mathbf{\Lambda}_6 - \bar{h}n_3\tilde{\boldsymbol{P}} + \bar{h}\boldsymbol{Z}_3,\quad \hat{\Xi}_{24}^{(1)} = \mathbf{\Lambda}_7, \\
\hat{\Xi}_{25}^{(1)} &= \mathbf{\Lambda}_8,\quad \hat{\Xi}_{33}^{(1)} = -\tilde{\gamma}_1^2 I,\ \hat{\Xi}_{34}^{(1)} = \mathbf{\Lambda}_{10}, \\
\hat{\Xi}_{35}^{(1)} &= \mathbf{\Lambda}_{11},\quad \hat{\Xi}_{44}^{(1)} = -\mathbf{\Lambda}_{13},\ \hat{\Xi}_{45}^{(1)} = \mathbf{\Lambda}_{14},\ \hat{\Xi}_{55}^{(1)} = \mathbf{\Lambda}_{15}, \\
\hat{\mathbf{\Psi}}_{21}^{(1)} &= \mathbf{\Lambda}_9,\quad \hat{\mathbf{\Psi}}_{31}^{(1)} = \mathbf{\Lambda}_{12}, \\
\mathbf{\Lambda}_1 &= \tilde{\boldsymbol{P}}(\boldsymbol{A}_i+\alpha\boldsymbol{I}) + (\boldsymbol{A}_i+\alpha\boldsymbol{I})^T\tilde{\boldsymbol{P}} + \boldsymbol{N}_1 + \boldsymbol{N}_1^T + \boldsymbol{I} \\
&\quad + \frac{\bar{h}^2}{4}m_3(\boldsymbol{A}_i+\alpha\boldsymbol{I})^T\tilde{\boldsymbol{P}}(\boldsymbol{A}_i+\alpha\boldsymbol{I}) + \frac{\bar{h}^2}{4}m_2\tilde{\boldsymbol{P}} \\
&\quad - n_1\tilde{\boldsymbol{P}}, \\
\mathbf{\Lambda}_2 &= -exp(\alpha\tau_2(t))\{\Upsilon_q\overline{\boldsymbol{K}}_j+\Upsilon_q^-\overline{\boldsymbol{F}}_j\} \\
&\quad - \frac{\bar{h}^2}{4}m_3 exp(\alpha\tau_2(t))(\boldsymbol{A}_i+\alpha\boldsymbol{I})^T\{\Upsilon_q\overline{\boldsymbol{K}}_j+\Upsilon_q^-\overline{\boldsymbol{F}}_j\} \\
&\quad - \frac{\bar{h}^2}{4}m_2\tilde{\boldsymbol{P}} + n_1\tilde{\boldsymbol{P}} - \boldsymbol{N}_1 + \boldsymbol{N}_2^T, \\
\mathbf{\Lambda}_3 &= -exp(\alpha\tau_2(t))\{\Upsilon_q\overline{\boldsymbol{K}}_j+\Upsilon_q^-\overline{\boldsymbol{F}}_j\} \\
&\quad - \frac{\bar{h}^2}{4}m_3 exp(\alpha\tau_2(t))(\boldsymbol{A}_i+\alpha\boldsymbol{I})^T\{\Upsilon_q\overline{\boldsymbol{K}}_j+\Upsilon_q^-\overline{\boldsymbol{F}}_j\}, \\
\mathbf{\Lambda}_4 &= -exp(\alpha\tau_2(t))\tilde{\boldsymbol{P}}\boldsymbol{E}_{fi} \\
&\quad - \frac{\bar{h}^2}{4}m_3 exp(\alpha\tau_2(t))(\boldsymbol{A}_i+\alpha\boldsymbol{I})^T\tilde{\boldsymbol{P}}\boldsymbol{E}_{fi}, \\
\mathbf{\Lambda}_5 &= \tilde{\boldsymbol{P}}\boldsymbol{E}_{di} + \frac{\bar{h}^2}{4}m_3(\boldsymbol{A}_i+\alpha\boldsymbol{I})^T\tilde{\boldsymbol{P}}\boldsymbol{E}_{di}, \\
\mathbf{\Lambda}_6 &= -n_1\tilde{\boldsymbol{P}} - \boldsymbol{N}_2 - \boldsymbol{N}_2^T + \frac{\bar{h}^2}{4}m_2\tilde{\boldsymbol{P}}, \\
\mathbf{\Lambda}_7 &= \frac{\bar{h}^2}{4}m_3 exp(2\alpha\tau_2(t))\{\Upsilon_q\overline{\boldsymbol{K}}_j^T+\Upsilon_q^-\overline{\boldsymbol{F}}_j^T\}\boldsymbol{E}_{fi}, \\
\mathbf{\Lambda}_8 &= -\frac{\bar{h}^2}{4}m_3 exp(\alpha\tau_2(t))\{\Upsilon_q\overline{\boldsymbol{K}}_j^T+\Upsilon_q^-\overline{\boldsymbol{F}}_j^T\}\boldsymbol{E}_{di}, \\
\mathbf{\Lambda}_9 &= \frac{\bar{h}^2}{4}m_3 exp(\alpha\tau_2(t))\{\Upsilon_q\overline{\boldsymbol{K}}_j^T+\Upsilon_q^-\overline{\boldsymbol{F}}_j^T\}, \\
\mathbf{\Lambda}_{10} &= \frac{\bar{h}^2}{4}m_3 exp(2\alpha\tau_2(t))\{\Upsilon_q\overline{\boldsymbol{K}}_j^T+\Upsilon_q^-\overline{\boldsymbol{F}}_j^T\}\boldsymbol{E}_{fi}, \\
\mathbf{\Lambda}_{11} &= -\frac{\bar{h}^2}{4}m_3 exp(\alpha\tau_2(t))\{\Upsilon_q\overline{\boldsymbol{K}}_j^T+\Upsilon_q^-\overline{\boldsymbol{F}}_j^T\}\boldsymbol{E}_{di}, \\
\mathbf{\Lambda}_{12} &= \frac{\bar{h}^2}{4}m_3 exp(\alpha\tau_2(t))\{\Upsilon_q\overline{\boldsymbol{K}}_j^T+\Upsilon_q^-\overline{\boldsymbol{F}}_j^T\}, \\
\mathbf{\Lambda}_{13} &= -\tilde{\gamma}_1^2\boldsymbol{I} - \frac{\bar{h}^2}{4}m_3 exp(2\alpha\tau_2(t))\boldsymbol{E}_{fi}^T\tilde{\boldsymbol{P}}\boldsymbol{E}_{fi}, \\
\mathbf{\Lambda}_{14} &= -\frac{\bar{h}^2}{4}m_3 exp(\alpha\tau_2(t))\boldsymbol{E}_{fi}^T\tilde{\boldsymbol{P}}\boldsymbol{E}_{di}, \\
\mathbf{\Lambda}_{15} &= -\tilde{\gamma}_1^2\boldsymbol{I} + \frac{\bar{h}^2}{4}m_3\boldsymbol{E}_{di}^T\tilde{\boldsymbol{P}}\boldsymbol{E}_{di}
\end{aligned}$$

Proof: We need to introduce the transformation* into the proof process to ensure that the closed-loop fault system possesses α-stability. The transformations are as follows, and (14) is equivalent to

$$\begin{cases}
\dot{\eta}(t) = \tilde{\boldsymbol{A}}_i\eta(t) - sat(\tilde{\boldsymbol{B}}_i\tilde{\boldsymbol{K}}_j\eta(t-\tau_2(t))) \\
\qquad - sat(\tilde{\boldsymbol{B}}_i\tilde{\boldsymbol{K}}_j e_\eta(t-\tau_2(t))) - \overline{\boldsymbol{E}}_{fi}e_{f_\alpha}(t-\tau_2(t)) \\
\qquad + \tau_2(t)\boldsymbol{E}_{fi}\dot{f}_\alpha(t) + \boldsymbol{E}_{di}d_\alpha(t) \\
y_\alpha(t) = \boldsymbol{C}_i\eta(t-\tau_2(t)) + v_\alpha(t_k)
\end{cases} \tag{35}$$

where $\tilde{\boldsymbol{A}}_i = \boldsymbol{A}_i + \alpha\boldsymbol{I}, \tilde{\boldsymbol{B}}_i\tilde{\boldsymbol{K}}_j = exp(\alpha\tau_2(t))\boldsymbol{B}_i\boldsymbol{K}_j$, and $\overline{\boldsymbol{E}}_{fi} = exp(\alpha\tau_2(t))\boldsymbol{E}_{fi}$.

We construct the Lyapunov-functional candidate as follows:

$$\begin{aligned}
V(\eta(t)) &= \eta^{\mathrm{T}}(t)\tilde{\boldsymbol{P}}\eta(t) \\
&\quad + (\bar{h}-\tau_2(t))\tau_2(t)\eta^T(t-\tau_2(t))\tilde{\boldsymbol{Q}}\eta(t-\tau_2(t)) \\
&\quad + (\bar{h}-\tau_2(t))\int_{t_k}^{t}\dot{\eta}^{\mathrm{T}}(s)\tilde{\boldsymbol{R}}\dot{\eta}(s)ds \\
&\quad + (\bar{h}-\tau_2(t))\overline{\eta}^{\mathrm{T}}(t)\tilde{\boldsymbol{S}}\overline{\eta}(t)
\end{aligned} \tag{36}$$

where $\tilde{\boldsymbol{P}} = \tilde{\boldsymbol{P}}^T > 0, \tilde{\boldsymbol{Q}} = \tilde{\boldsymbol{Q}}^T > 0, \tilde{\boldsymbol{R}} = \tilde{\boldsymbol{R}}^T > 0, \tilde{\boldsymbol{S}} = \tilde{\boldsymbol{S}}^T > 0$, and $\overline{\eta}(t) = \eta(t) - \eta(t_k)$.

Firstly, we prove the system with α-stability. We set that $e_\eta(t-\tau_2(t)) = 0, e_{f_\alpha}(t-\tau_2(t)) = 0, d_\alpha(t) = 0,$

and $v_\alpha(t_k) = 0$. Along with the trajectory of (35), we obtain (37) by calculating the derivative of $V(\eta(t))$.

$$\begin{aligned}\dot{V}(\eta(t)) = & 2\eta^{\mathrm{T}}(t)\tilde{\boldsymbol{P}}\dot{\eta}(t) \\ & -\bar{h}\eta^T(t-\tau_2(t))\tilde{\boldsymbol{Q}}\eta(t-\tau_2(t)) \\ & +2(\bar{h}-\tau_2(t))\eta^T(t-\tau_2(t))\tilde{\boldsymbol{Q}}\eta(t-\tau_2(t)) \\ & -\int_{t_k}^{t}\dot{\eta}^{\mathrm{T}}(s)\tilde{\boldsymbol{R}}\dot{\eta}(s)ds \\ & +(\bar{h}-\tau_2(t))\dot{\eta}^{\mathrm{T}}(t)\tilde{\boldsymbol{R}}\dot{\eta}(t)-\overline{\eta}^{\mathrm{T}}(t)\tilde{\boldsymbol{S}}\overline{\eta}(t) \\ & +2(\bar{h}-\tau_2(t))\overline{\eta}^{\mathrm{T}}(t)\tilde{\boldsymbol{S}}\dot{\eta}(t)\end{aligned} \quad (37)$$

For the actuator saturation constraints, we make the following definition by applying Lemma 1 of [15]. $\eta(t) = \tilde{\boldsymbol{M}}_1\tilde{\xi}(t), \overline{\eta}(t) = \tilde{\boldsymbol{M}}_2\tilde{\xi}(t), \dot{\eta}(t) = \tilde{\boldsymbol{M}}_3\tilde{\xi}(t) + \tau_2(t)\cdot\boldsymbol{E}_f\dot{f}_\alpha(t)$, $\eta(t-\tau_2(t)) = \eta(t_k) = \tilde{\boldsymbol{M}}_4\tilde{\xi}(t)$, where $\tilde{\xi}(t) = \left[\eta^T(t),\ \eta^T(t_k)\right], \tilde{\boldsymbol{M}}_1 = [\boldsymbol{I}\ 0], \tilde{\boldsymbol{M}}_2 = [\boldsymbol{I}\ -\boldsymbol{I}], \tilde{\boldsymbol{M}}_3 = \left[\tilde{\boldsymbol{A}}_i - \tilde{\boldsymbol{B}}_i co\{\Upsilon_q\tilde{\boldsymbol{K}}_j + \Upsilon_q^-\tilde{\boldsymbol{F}}_j\}\right], \tilde{\boldsymbol{M}}_4 = [0\ \boldsymbol{I}]$.

We express the $\overline{\eta}(t)$ as

$$\overline{\eta}(t) = \eta(t) - \eta(t_k) = \int_{t_k}^{t}\dot{\eta}(s)ds \quad (38)$$

We deal with the integral item $-\int_{t_k}^{t}\dot{\eta}^T(s)\tilde{\boldsymbol{R}}\dot{\eta}(s)ds$ of $\dot{V}(t)$ based on the Schur complement Lemma, Cauchy's inequality and Jensen's inequality, and we get

$$-\int_{t_k}^{t}\dot{\eta}^T(s)\tilde{\boldsymbol{R}}\dot{\eta}(s)ds \le 2\tilde{\xi}^T(t)\tilde{\boldsymbol{N}}\overline{\eta}(t) + \tau_2(t)\tilde{\xi}^T(t)\tilde{\boldsymbol{Z}}\tilde{\xi}(t) \quad (39)$$

where $\tilde{\boldsymbol{R}} \in R^{n\times n}, \tilde{\boldsymbol{N}} \in R^{2n\times n}, \tilde{\boldsymbol{Z}} \in R^{2n\times 2n}$ satisfy (32-c).

Combined with the Lemma 1 of [15] and (39), (37) is equivalent to

$$\begin{aligned}\dot{V}(t) \le \max_{i\in[1,2,\cdots,2^m]} & \{\tilde{\xi}^T(t)[2\tilde{\boldsymbol{M}}_1^T\tilde{\boldsymbol{P}}\tilde{\boldsymbol{M}}_3 - \bar{h}\tilde{\boldsymbol{M}}_4^T\tilde{\boldsymbol{Q}}\tilde{\boldsymbol{M}}_4 \\ & -\tilde{\boldsymbol{M}}_2^T\tilde{\boldsymbol{S}}\tilde{\boldsymbol{M}}_2 + 2\tilde{N}\tilde{\boldsymbol{M}}_2 + (\bar{h}-\tau_2(t))(2\tilde{\boldsymbol{M}}_4^T\tilde{\boldsymbol{Q}}\tilde{\boldsymbol{M}}_4 \\ & +\tilde{\boldsymbol{M}}_3^T\tilde{\boldsymbol{R}}\tilde{\boldsymbol{M}}_3 + 2\tilde{\boldsymbol{M}}_2^T\tilde{\boldsymbol{S}}\tilde{\boldsymbol{M}}_3) + \tau_2(t)\tilde{\boldsymbol{Z}}]\tilde{\xi}(t) \\ & +2\tau_2(t)\eta^T(t)\tilde{\boldsymbol{P}}\boldsymbol{E}_{fi}\dot{f}_\alpha(t) \\ & +2(\bar{h}-\tau_2(t))(\overline{\eta}^T(t)\tilde{\boldsymbol{S}}\boldsymbol{E}_{fi}\dot{f}_\alpha(t) \\ & +\tilde{\xi}^T(t)\tilde{\boldsymbol{M}}_3^T\tilde{\boldsymbol{R}}\boldsymbol{E}_{fi}\dot{f}_\alpha(t)) \\ & +(\bar{h}-\tau_2(t))\tau_2^2(t)\dot{f}_\alpha^T(t)\boldsymbol{E}_f^T\tilde{\boldsymbol{R}}\boldsymbol{E}_f\dot{f}_\alpha(t)\}\end{aligned} \quad (40)$$

According to (32-d, e, f) and Moon's inequality, we obtain

$$\begin{aligned}2\tau_2(t)\eta^T(t)\tilde{\boldsymbol{P}}\boldsymbol{E}_{fi}\dot{f}_\alpha(t) & \le \tau_2(t)\eta^T(t)\boldsymbol{Q}_2\eta(t) \\ & +\bar{h}f_0^2\lambda_{\max}(\boldsymbol{Q}_1)\end{aligned} \quad (41)$$

$$\begin{aligned}2(\bar{h}-\tau_2(t))\overline{\eta}^T(t)\tilde{\boldsymbol{S}}\boldsymbol{E}_{fi}\dot{f}_\alpha(t) & \le \frac{\bar{h}^2}{4}\overline{\eta}^T(t)\boldsymbol{Q}_4\overline{\eta}(t) \\ & +\frac{\bar{h}^2}{4}f_0^2\lambda_{\max}(\boldsymbol{Q}_3)\end{aligned} \quad (42)$$

$$\begin{aligned}2(\bar{h}-\tau_2(t))\tilde{\xi}^T(t)\tilde{\boldsymbol{M}}_3^T\tilde{\boldsymbol{R}}\boldsymbol{E}_{fi}\dot{f}_\alpha(t) \le \frac{\bar{h}^2}{4}\tilde{\xi}^T(t)\tilde{\boldsymbol{M}}_3^T\boldsymbol{Q}_6\tilde{\boldsymbol{M}}_3\tilde{\xi}(t) + \frac{\bar{h}^2}{4}f_0^2\lambda_{\max}(\boldsymbol{Q}_5)\end{aligned} \quad (43)$$

$$\begin{aligned}(\bar{h}-\tau_2(t))\tau_2^2(t)\dot{f}_\alpha^T(t)\boldsymbol{E}_{fi}^T\tilde{\boldsymbol{R}}\boldsymbol{E}_{fi}\dot{f}_\alpha(t) \le \frac{\bar{h}^3}{8}f_0^2\lambda_{\max}(\boldsymbol{E}_{fi}^T\tilde{\boldsymbol{R}}\boldsymbol{E}_{fi})\end{aligned} \quad (44)$$

We get (45) by applying (41)–(43) into (40).

$$\begin{aligned}\dot{V}(t) \le \max_{i\in[1,2,\cdots,2^m]} & \{\tilde{\xi}^T(t)[\tilde{\boldsymbol{\Gamma}}_1 + (\bar{h}-\tau_2(t))\tilde{\boldsymbol{\Gamma}}_2 \\ & +\tau_2(t)\tilde{\boldsymbol{\Gamma}}_3]\tilde{\xi}(t)\} + \delta\end{aligned} \quad (45)$$

where

$$\begin{aligned}\tilde{\boldsymbol{\Gamma}}_1 &= 2\tilde{\boldsymbol{M}}_1^T\tilde{\boldsymbol{P}}\tilde{\boldsymbol{M}}_3 - \bar{h}\tilde{\boldsymbol{M}}_4^T\tilde{\boldsymbol{Q}}\tilde{\boldsymbol{M}}_4 - \tilde{\boldsymbol{M}}_2^T\tilde{\boldsymbol{S}}\tilde{\boldsymbol{M}}_2 + 2\tilde{\boldsymbol{N}}\tilde{\boldsymbol{M}}_2 \\ &\quad + \frac{\bar{h}^2}{4}\tilde{\boldsymbol{M}}_2^T\boldsymbol{Q}_4\tilde{\boldsymbol{M}}_2 + \frac{\bar{h}^2}{4}\tilde{\boldsymbol{M}}_3^T\boldsymbol{Q}_6\tilde{\boldsymbol{M}}_3 \\ \tilde{\boldsymbol{\Gamma}}_2 &= 2\tilde{\boldsymbol{M}}_4^T\tilde{\boldsymbol{Q}}\tilde{\boldsymbol{M}}_4 + \tilde{\boldsymbol{M}}_3^T\tilde{\boldsymbol{R}}\tilde{\boldsymbol{M}}_3 + 2\tilde{\boldsymbol{M}}_2^T\tilde{\boldsymbol{S}}\tilde{\boldsymbol{M}}_3, \\ \tilde{\boldsymbol{\Gamma}}_3 &= \tilde{\boldsymbol{Z}} + \tilde{\boldsymbol{M}}_1^T\boldsymbol{Q}_2\tilde{\boldsymbol{M}}_1, \\ \delta &= \bar{h}f_0^2\lambda_{max}(\boldsymbol{Q}_1) + \frac{\bar{h}^2}{4}f_0^2\lambda_{max}(\boldsymbol{Q}_2) \\ &\quad + \frac{\bar{h}^2}{4}f_0^2\lambda_{max}(\boldsymbol{Q}_5) + \frac{\bar{h}^2}{8}f_0^2\lambda_{max}(\boldsymbol{E}_{fi}^T\tilde{\boldsymbol{R}}\boldsymbol{E}_{fi})\end{aligned}$$

In (45), if $\tilde{\boldsymbol{\Gamma}}_1 + (\bar{h}-\tau_2(t))\tilde{\boldsymbol{\Gamma}}_2 + \tau_2(t)\tilde{\boldsymbol{\Gamma}}_3 < 0$, then $\dot{V}(t) \le -\varepsilon\left\|\tilde{\xi}(t)\right\|^2 + \delta$, where $\varepsilon = \lambda_{\min}[-(\tilde{\boldsymbol{\Gamma}}_1 + (\bar{h}-\tau_2(t))\tilde{\boldsymbol{\Gamma}}_2 + \tau_2(t)\tilde{\boldsymbol{\Gamma}}_3)]$. Therefore, $\dot{V}(t) < 0$ when $\varepsilon\left\|\tilde{\xi}(t)\right\|^2 > \delta$. In terms of Lyapunov stability theory, $\tilde{\xi}(t)$ will eventually converge to the set $\Psi = \{\tilde{\xi}(t)|\left\|\tilde{\xi}(t)\right\|^2 < {}^{\delta}/_{\varepsilon}\}$, and the system (35) is uniformly and ultimately bounded.

Due to space limitation, we omit the proof process of performance index H_∞/H_2 in Theorem 2. The proof method is similar to [8], to which interested readers can refer.

V. SIMULATION AND EXPERIMENT

Considering the nonlinear NCSs model [17], we set the fuzzy membership function as $M_1(x_4) = sin^2x_4$, $M_2(x_4) = cos^2x_4$, $M_3(x_4) = sin^2x_4$, and $M_4(x_4) = cos^2x_4$. And then we can express the nonlinear system as a T-S fuzzy system with 4 rules.

$$\text{Rule i}: \text{ if } x_4 \text{ is } M_i, i = 1,2,3,4, \text{ then} \\ \begin{cases}\dot{x}(t) = \boldsymbol{A}_ix(t) + \boldsymbol{B}_isat(u(t)) + \boldsymbol{E}_{di}d(t) + \boldsymbol{E}_{fi}f(t) \\ y(i_k) = \boldsymbol{C}_ix(i_k) + \boldsymbol{D}_{vi}v(i_k)\end{cases}$$

$$\boldsymbol{A}_1 = \begin{bmatrix}-0.016 & 0 & 0.042 & 0 \\ 0 & -0.011 & 0 & 0.033 \\ 0 & 0 & -0.042 & 0 \\ 0 & 0 & 0 & -0.033\end{bmatrix},$$

$$\boldsymbol{A}_2 = \begin{bmatrix}-0.022 & 0 & 0.061 & 0 \\ 0 & -0.018 & 0 & 0.049 \\ 0 & 0 & -0.064 & 0 \\ 0 & 0 & 0 & -0.049\end{bmatrix},$$

$$\boldsymbol{A}_3 = \begin{bmatrix}-0.031 & 0 & 0.053 & 0 \\ 0 & -0.021 & 0 & 0.067 \\ 0 & 0 & -0.083 & 0 \\ 0 & 0 & 0 & -0.061\end{bmatrix},$$

$$A_4 = \begin{bmatrix} -0.039 & 0 & 0.106 & 0 \\ 0 & -0.0276 & 0 & 0.0826 \\ 0 & 0 & -0.107 & 0 \\ 0 & 0 & 0 & -0.0827 \end{bmatrix},$$

$$B_1 = \begin{bmatrix} 0.083 & 0 \\ 0 & 0.063 \\ 0 & 0.048 \\ 0.031 & 0 \end{bmatrix}, \quad B_2 = \begin{bmatrix} 0.1246 & 0 \\ 0 & 0.093 \\ 0 & 0.071 \\ 0.045 & 0 \end{bmatrix},$$

$$B_3 = \begin{bmatrix} 0.165 & 0 \\ 0 & 0.125 \\ 0 & 0.097 \\ 0.063 & 0 \end{bmatrix}, \quad B_4 = \begin{bmatrix} 0.2076 & 0 \\ 0 & 0.1576 \\ 0 & 0.13 \\ 0.0776 & 0 \end{bmatrix},$$

$$E_{d4} = \begin{bmatrix} 0.024 \\ 0.024 \\ 0 \\ 0.024 \end{bmatrix}, \quad E_{f1} = -\begin{bmatrix} 0.083 & 0 & 0 & 0.031 \end{bmatrix}^T,$$

$$E_{f2} = -\begin{bmatrix} 0.1246 & 0 & 0 & 0.0464 \end{bmatrix}^T,$$
$$E_{f3} = -\begin{bmatrix} 0.167 & 0 & 0 & 0.061 \end{bmatrix}^T,$$
$$E_{f4} = -\begin{bmatrix} 0.2076 & 0 & 0 & 0.0774 \end{bmatrix}^T,$$
$$C_1 = diag\{0.5 \quad 0.5 \quad 0.5 \quad 0.5\},$$
$$C_2 = diag\{0.48 \quad 0.48 \quad 0.48 \quad 0.48\},$$
$$C_3 = diag\{0.46 \quad 0.46 \quad 0.46 \quad 0.46\},$$
$$C_4 = diag\{0.52 \quad 0.52 \quad 0.52 \quad 0.52\},$$
$$D_{v1} = \begin{bmatrix} 0.015 & 0 & 0.015 & 0.015 \end{bmatrix}^T,$$
$$D_{v2} = \begin{bmatrix} 0.0224 & 0 & 0.0224 & 0.0224 \end{bmatrix}^T,$$
$$D_{v3} = \begin{bmatrix} 0.030 & 0 & 0.025 & 0.027 \end{bmatrix}^T,$$
$$D_{v4} = \begin{bmatrix} 0.0374 & 0 & 0.031 & 0.0326 \end{bmatrix}^T,$$
$$f(t) = \begin{cases} 0 & t \le 100s \\ 2 + 2sin0.01\pi(t-100) & 100s < t \le 800s \end{cases}$$

The model parameters satisfy the related condition, which is $rank(B_i, E_{f_i}) = rank(B_i)$. We assume that the disturbance $d(t)$ and $v(t_k)$ are the white noise process and the sequence, and the zero mean variance of $d(t)$ and $v(t_k)$ are 0.01. We set $x_{01} = x_{02} = x_{03} = x_{04} = [4\ 4\ 2\ 2]^T$. We suppose $n_1 = 1.1, n_2 = 0.8, n_3 = 0.6, h = 0.1$.

From Theorem 1, we obtain $\gamma_{1min} = 5.6789$ and the following result:

$$L_1 = \begin{bmatrix} 17.1631 & 4.6602 & 12.7101 & -41.7562 \\ 0.6223 & 2.7123 & 1.1516 & -1.7234 \\ 0.13231 & -0.0604 & 1.1553 & 0.3123 \\ 5.9603 & 1.8345 & 4.8765 & -13.9876 \end{bmatrix},$$

$$L_2 = \begin{bmatrix} 15.9487 & 11.7892 & 18.9750 & -35.4576 \\ 0.6079 & 2.8764 & 0.8749 & -1.4483 \\ 0.1843 & -0.1741 & 1.0773 & -0.3978 \\ 5.5872 & 4.5602 & 7.1321 & -12.0123 \end{bmatrix},$$

$$L_3 = \begin{bmatrix} 19.9478 & 5.8720 & 25.9765 & -44.5872 \\ 0.8116 & 3.3356 & 1.3212 & -1.7921 \\ 0.0502 & -0.1695 & 0.6123 & -0.0325 \\ 7.0897 & 2.4732 & 9.8343 & -15.6760 \end{bmatrix},$$

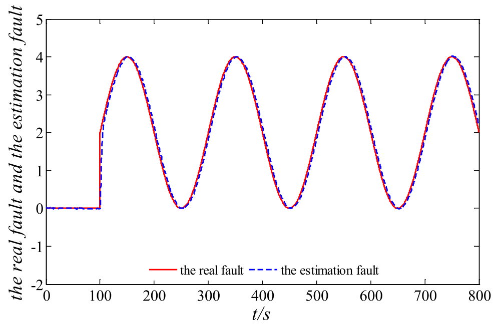

FIGURE 2. The trend of variation of continuous time-varying fault and its estimation value on the experimental platform.

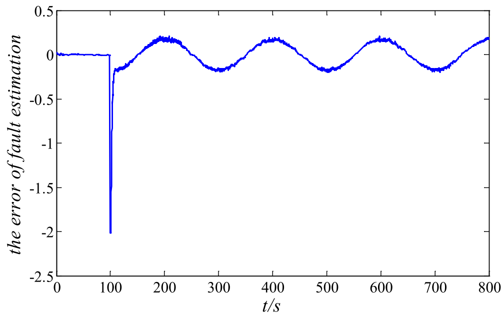

FIGURE 3. The variation of error for the estimation fault value.

$$L_4 = \begin{bmatrix} 19.2322 & 10.7654 & 24.0033 & -43.1678 \\ 0.5923 & 3.0437 & 0.8678 & -1.4987 \\ -0.0367 & -1.0427 & 0.3823 & 0.1874 \\ 6.8724 & 4.2234 & 8.5123 & -15.5234 \end{bmatrix},$$
$$F_1 = \begin{bmatrix} -26.9503 & 108.712 & -1.7876 & 41.2567 \end{bmatrix},$$
$$F_2 = \begin{bmatrix} -28.8765 & 4.5678 & 7.3456 & -12.9876 \end{bmatrix},$$
$$F_3 = \begin{bmatrix} -37.7865 & 116.8765 & -50.2945 & 63.3456 \end{bmatrix},$$
$$F_4 = \begin{bmatrix} -25.4567 & 112.5678 & -35.7658 & 39.7654 \end{bmatrix}$$

A. SIMULATION VERIFICATION

In this section, we carry out the simulation based on the stand-alone version of MATLAB. The changing tendency of continuous time-varying fault estimation and its estimation error are shown in Figure 2 and Figure 3.

From Figure 2 and Figure 3, we obtain that the fault observer designed by Theorem 1 can estimate the continuous time-varying fault accurately, and the error variation of fault-estimation will be smaller. The observer based on Theorem 1 has a smaller error compared with the result of [17]. Apart from the moment when the fault occurs, the error in the remaining instants will remain within 0.2. However, the corresponding result of [17] will be larger than 0.2. According to $(I - B_i B_j^{+})E_{fi} = 0$, the non-uniform transmission fault-accommodation active fault-tolerant controllers are obtained as follows:

$$B_1^{+} = \begin{bmatrix} 12.7654 & -11.3247 & 0 & 0.3456 \\ 0 & 0 & 0 & 0 \end{bmatrix},$$

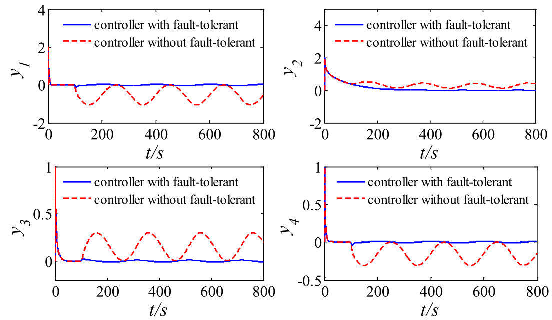

FIGURE 4. The trend of output for the closed-loop system.

$$\boldsymbol{B}_2^+ = \begin{bmatrix} 7.8765 & -7.7865 & 0 & 0.2345 \\ 0 & 0 & 0 & 0 \end{bmatrix},$$
$$\boldsymbol{B}_3^+ = \begin{bmatrix} 5.8325 & -5.3456 & 0 & 0.1324 \\ 0 & 0 & 0 & 0 \end{bmatrix},$$
$$\boldsymbol{B}_4^+ = \begin{bmatrix} 4.7654 & -4.2543 & 0 & 0.0897 \\ 0 & 0 & 0 & 0 \end{bmatrix}$$

After the continuous time-varying fault is estimated accurately, we adopt the non-uniform transmission active fault-tolerant controller to accommodate the fault based on Theorem 2. We set some related parameters as follows: $h = 0.1, n_1 = 1.1, n_2 = 0.95, n_3 = 0.2, m_1 = 0.2, m_2 = 0.1, m_3 = 0.2, \bar{h} = 1.0, \alpha = 0.2, \tilde{\gamma}_1 = 1.6, \tilde{\gamma}_2 = 1.6, \delta = 0.00005$, Υ_1=[1 0 0 0 ; 0 0 0 0; 0 0 0 0; 0 0 0 0], Υ_2=[0 0 0 0 ; 0 1 0 0; 0 0 0 0; 0 0 0 1]. According to the integrated design method in Theorem 2, the state feedback controller with fault accommodation ability and event-triggered weight matrix are as follows:

$$\boldsymbol{K}_1 = \begin{bmatrix} 4.6758 & -0.0631 & 0.3245 & -0.1476 \\ 1.0476 & 0.2134 & 5.9133 & 0.2432 \end{bmatrix},$$
$$\boldsymbol{K}_2 = \begin{bmatrix} 3.2345 & -0.0456 & 0.2134 & -0.0978 \\ 0.7233 & 0.1513 & 4.0224 & 0.1567 \end{bmatrix},$$
$$\boldsymbol{K}_3 = \begin{bmatrix} 2.3157 & -0.0198 & 0.1876 & -0.0756 \\ 0.5137 & 0.1067 & 3.0578 & 0.1123 \end{bmatrix},$$
$$\boldsymbol{K}_4 = \begin{bmatrix} 1.8765 & -0.0197 & 0.1765 & -0.0498 \\ 0.4123 & 0.0789 & 2.3245 & 0.0797 \end{bmatrix},$$
$$\boldsymbol{\Phi} = diag\left\{ 188.7654 \quad 186.7654 \quad 195.6543 \quad 197.7754 \right\}$$

Under the combined effects of $\boldsymbol{K}_j$, $\boldsymbol{B}_j^+$and $\boldsymbol{\Phi}$, the system output of (14) are shown in Figure 4.

Figure 4 presents two kinds of system output curves. When the system has a time-varying fault, the controller without a fault-tolerant tolerant ability will lead to the system output having larger fluctuation. Obviously, when we adopt the non-uniform transmission fault-tolerant controller based on Theorem 2, the closed-loop fault system with actuator saturation will possess good dynamic performance. The controller is designed by considering the α-stability and the generalised H_2/H_∞performance index. Compared with the output response of the system in [17], we find that the attenuation speed of the output response in Figure 4 is faster, which is due to the satisfactory active fault-tolerant control in this paper, i.e. meeting multiple performance indicators (such as the α-stability and the generalised H_2/H_∞ performance index). Due to space limitation, the output response in [17] is not given here. For further information, please refer to [17].

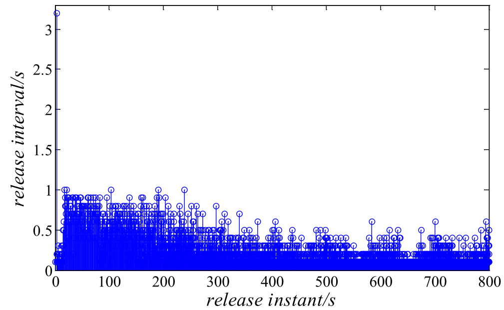

FIGURE 5. The data transmission details of the fault system.

TABLE 1. System data transmission details under different event-triggered parameters.

δ	0.00001	0.00003	0.00005	0.00007	0.00009
n	5987	4987	4413	4123	3877
$r_{e/t}$	74.84%	62.34%	55.16%	51.54%	48.46%
h_{av}	0.1321	0.1611	0.1798	0.1977	0.2099

(n denotes the quantity of transmission data selected by the event-generator. $r_{e/t}$ indicates the ratio of the amount of transmission data in DETCS and the amount of transmission data in PTTCS; h_{av} expresses the average transmission period.)

Under DETCS, the data transmission details of closed-loop fault system (14) is shown in Figure 5.

When we adopt the PTTCS driven by the clock, the system will transmit 8000 pieces of data. From Figure 5, we find that the amount of data sent has decreased, and the system will transmit 4515 pieces of data by statistical calculation under DETCS. Compared with PTTCS, the amount of data sent is reduced by 3485. Therefore the DETCS can save a certain quantity of network communication resource. While saving network resource, the integrated design method also ensures that the closed-loop system has good performance, which is due to the consideration of the satisfactory active fault-tolerant control (such as the α-stability and the generalised H_2/H_∞ performance index) in this paper.

When we select different values for event-triggered parameter δ, we still set 800s as the simulation time. The data transmission details for nonlinear NCSs with the fault-tolerant ability are shown in Table 1.

As the event-triggered parameter becomes large, the average transmission period h_{av}will also increase, as shown in Table 1, while the data transmission ratio $r_{e/t}$ and data transmission quantity n will be reduced. The trade-off between the system control quality and network service quality is achieved by adjusting the event-triggered parameter.

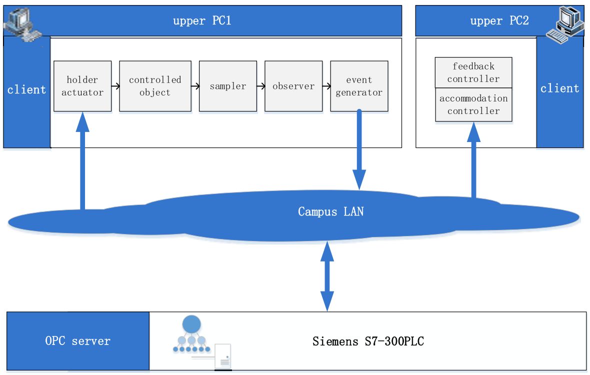

FIGURE 6. The semi entity experimental platform for NCSs.

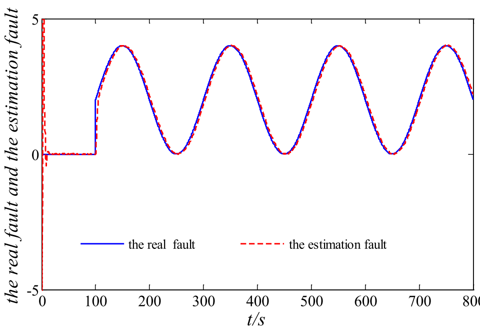

FIGURE 7. The trend of variation of continuous time-varying fault and its estimation value on the experimental platform.

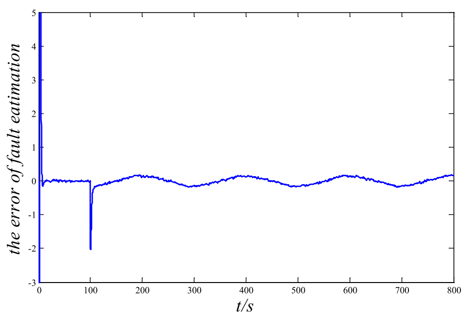

FIGURE 8. The variation of error for the estimation fault value on the experimental platform.

B. EXPERIMENTAL PLATFORM VERIFICATION

In order to fully reflect the real network transmission details, this section will verify the feasibility of the above theory result using the active fault-tolerant semi entity experimental platform. Based on the campus LAN, the Siemens S7-300 PLC, Step 7, SimaticNet and MATLAB 7.10, we establish the active fault-tolerant semi entity experimental platform under DETCS by adopting the OLE for the process control system. The sketch diagram is shown in Figure 6.

The experimental platform verification is carried out by using the numerical example of *A. SIMULATION VERIFICATION*. The variation of fault-estimation and the error of fault-estimation for nonlinear NCSs with time-varying faults are shown in Figure 7 and Figure 8, and the system output and control input are shown in Figure 9 and Figure 10.

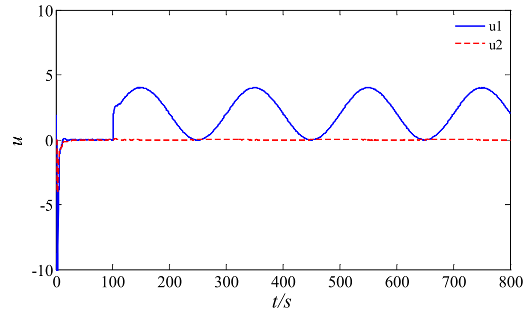

FIGURE 9. The trend of variation of control input on the experimental platform.

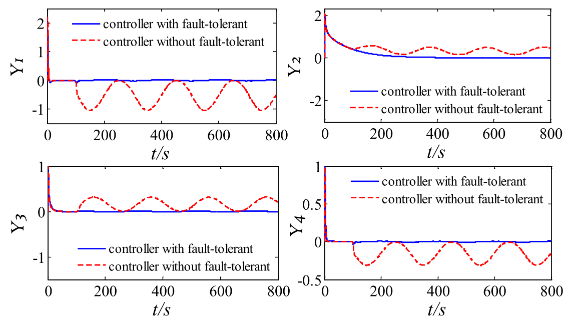

FIGURE 10. The trend of output for the closed-loop system on the experimental platform.

TABLE 2. Data transmission details for non-uniform transmission nonlinear NCSs under different experimental environments.

Experimental environment	n	h_{av}	$r_{e/t}$
Stand-alone version simulation under PTTCS	8000	0.1	100%
Stand-alone version simulation under DETCS	5987	0.1321	74.84%
Experimental platform under DETCS	6219	0.1312	77.73%

From Figure 7 and Figure 8, we can conclude that the fault estimation method with H_∞-performance in section III is effective and feasible, and its error is slightly higher than the simulation results under the stand-alone version of MATLAB. From the system output curve in Figure 9, we can see that in the real network transmission environment the event-triggered method presented in Section IV is reliable and effective. This method can guarantee that the closed-loop fault NCSs not only process the asymptotic stability but also process the α-stability and the generalised H_∞/H_2-performance.

Table 2 presents the data transmission details of the nonlinear closed-loop fault system (14) with multi-objective constraints in three cases of 800s: the stand-alone version simulation under PTTCS, the stand-alone version simulation under DETCS, and the experiment platform under DETCS.

From Table 2, we find that in the 800s simulation time network communication resource will be saved effectively under DETCS. Compared with the stand-alone version experiment, the performance of the closed-loop fault system is slightly worse, and the occupancy rate of the network communication resource is slightly bigger because of the time-delay and disorder problem in real network.

VI. CONCLUSION

For nonlinear NCSs with actuator saturation and continuous time-varying faults, the problem of a satisfactory integrated design combining active fault-tolerant control and network communication saving was studied in this paper. The effect of the non-uniform transmission period on the performance of the nonlinear NCSs under DETCS is transformed into the time-delay of the system by applying the study method of a non-uniform sampled-data system. Firstly, based on Lyapunov theory and linear convex combination theory, the fault estimation method with H_∞-performance is presented by adopting the continuous time state observer under equal physical sampling period. Furthermore, under the non-uniform transmission period, a method for solving the integrated design is proposed under DETCS, and we can obtain a satisfactory active fault-tolerant controller and event-triggered weight matrix simultaneously through the integrated design method. The closed-loop system fault possesses α-stability, H_2-performance, and H_∞-performance when adopting a satisfactory active fault-tolerant controller, even if the actuator is subject to saturation constraints. By adopting a nonlinear simulation example, the simulation and experimental platform results show that the method is more accurate than those previously reported in the literature. Moreover, the method ensures that the closed-loop system not only possesses good dynamic performance but can also save a certain amount of network communication resource under the given event-triggered condition, which can achieve a trade-off between system control quality and network service quality for nonlinear NCSs.

REFERENCES

[1] R. J. Patton, C. Kambhampati, A. Casavola, and G.Franzè, "Fault-tolerance as a key requirement for the control of modern systems," *Int. Fed. Autom. Control Proc.*, vol. 39, no. 13, pp. 13–22, Apr. 2006.

[2] C. Liu, K. Lu, J. Sun, and J. Dai, "Fault tolerant control with disturbance estimator for a class of linear parameter varying systems subject to time-varying fault," *Trans. Inst. Meas. Control*, vol. 41, no. 13, pp. 3836–3846, Sep. 2019.

[3] C. Peng, E. G. Tian, and T. C. Yang, "Robust fault-tolerant control of networked control systems with stochastic actuator failure," *IET Control Theory Appl.*, vol. 4, no. 12, pp. 3003–3011, Dec. 2010.

[4] M. Bahreini, J. Zarei, R. Razavi-Far, and M. Saif, "Robust finite-time stochastic stabilization and fault-tolerant control for uncertain networked control systems considering random delays and probabilistic actuator faults," *Trans. Inst. Meas. Control*, vol. 41, no. 12, pp. 3550–3561, Aug. 2019.

[5] H. Yang, B. Jiang, and D. H. Zhou, "Review and perspectives on fault tolerant control for interconnected systems," *Acta Automatica Sinica*, vol. 43, no. 1, pp. 9–19, Jan. 2017.

[6] M. S. Mahmoud, A. M. Memon, and P. Shi, "Observer-based fault-tolerant control for a class of nonlinear networked control systems," *Int. J. Control*, vol. 87, no. 8, pp. 1707–1715, Aug. 2014.

[7] X. Chu and M. Li, "Event-triggered fault estimation and sliding mode fault-tolerant control for a class of nonlinear networked control systems," *J. Franklin Inst.*, vol. 355, no. 13, pp. 5475–5502, Sep. 2018.

[8] W. Li and F. Y. Shen, "Satisfactory fault-tolerant design of NCS with α-stability," *Control Eng. China*, vol. 20, no. 1, pp. 149–154, Jan. 2013.

[9] Y. J. Li and W. Li, "Co-design between satisfactory fault-tolerant control for NCS with actuator saturation and communication," *J. Huazhong Univ. Sci. Technol., Natural Sci. Ed. China*, vol. 45, no. 1, pp. 69–75, Jan. 2017.

[10] D. Yue, E. Tian, and Q.-L. Han, "A delay system method for designing event-triggered controllers of networked control systems," *IEEE Trans. Autom. Control*, vol. 58, no. 2, pp. 475–481, Feb. 2013.

[11] X. You, C. Hua, and X. Guan, "Event-triggered leader-following consensus for nonlinear multiagent systems subject to actuator saturation using dynamic output feedback method," *IEEE Trans. Autom. Control*, vol. 63, no. 12, pp. 4391–4396, Dec. 2018.

[12] Y. Wang, G. Song, and J. Zhao, "Reliable mixed H_∞ and passive control for networked control systems under adaptive event-triggered scheme with actuator faults and randomly occurring nonlinear perturbations," *ISA Trans.*, vol. 89, no. 6, pp. 45–57, Jun. 2019.

[13] J. Liu and D. Yue, "Event-triggering in networked systems with probabilistic sensor and actuator faults," *Inf. Sci.*, vol. 240, pp. 145–160, Aug. 2013.

[14] K. Duan and W. Zhang, "Event-triggered fault-tolerant control for networked systems with dynamic quantiser," *IET Control Theory Appl.*, vol. 10, no. 9, pp. 1088–1096, Jun. 2016.

[15] H.-C. Cao and W. Li, "Robust fault-tolerant control for uncertain NNCS with discrete event-triggered communication scheme," *J. Jilin Univ., Eng. Technol. Ed.*, vol. 45, no. 6, pp. 1895–1905, Nov. 2015.

[16] H. Li, Z. Chen, L. Wu, H.-K. Lam, and H. Du, "Event-triggered fault detection of nonlinear networked systems," *IEEE Trans. Cybern.*, vol. 47, no. 4, pp. 1041–1052, Apr. 2017.

[17] A. B. Qiu, H. G. Ji, and J. P. Gu, "Optimal integrated design of time-varying fault estimation and accommodation for nonuniformly sampled data systems," *Acta Automatica Sinica*, vol. 40, no. 7, pp. 1493–1504, Jul. 2014.

[18] Z. Mao, B. Jiang, and P. Shi, "Fault detection for a class of nonlinear networked control systems," *Int. J. Adapt. Control Signal Process.*, vol. 24, no. 7, pp. 610–622, Jul. 2010.

[19] W. Wu and Y. Zhang, "Event-triggered fault-tolerant control and scheduling codesign for nonlinear networked control systems with medium-access constraint and packet disordering," *Int. J. Robust Nonlinear Control*, vol. 28, no. 4, pp. 1182–1198, Mar. 2018.

[20] H. Q. Xiao, M. Wu, Y. He, and S.-P. Xiao, "H_∞ output tracking control for sampled-data networked control systems in T-S fuzzy model," *Acta Automatica Sinica*, vol. 41, no. 3, pp. 661–668, Mar. 2015.

[21] E. Fridman and Y. Orlov, "Exponential stability of linear distributed parameter systems with time-varying delays," *Automatica*, vol. 45, no. 1, pp. 194–201, Jan. 2009.

[22] F. Yang, H. Zhang, and Y. Wang, "An enhanced input-delay approach to sampled-data stabilization of T-S fuzzy systems via mixed convex combination," *Nonlinear Dyn.*, vol. 75, no. 3, pp. 501–512, Feb. 2014.

YAJIE LI was born in Puyang, Henan, China, in 1981. She received the Ph.D. degree in control theory and control engineering from the Lanzhou University of Technology, Lanzhou, China, in 2017. She is currently a Lecturer with the College of Electrical and Information Engineering, Lanzhou University of Technology. She is mainly engaged in fault diagnosis and fault tolerant control.

WEI LI was born in Xi'an, Shanxi, China, in 1963. She is currently a Professor and a Ph.D. Candidate Tutor with the College of Electrical and Information Engineering, Lanzhou University of Technology. Her research interests include fault diagnosis, fault-tolerant control, and attack tolerance control.